



**TRIBHUVAN UNIVERSITY
INSTITUTE OF ENGINEERING
PULCHOWK CAMPUS**

THESIS NO.: 078/MSCCD/012

**Analyzing the Hydrological Regime of Sunkoshi River Basin, Nepal, using a Glacio-
hydrological Degree-day Model (GDM)**

by

SAILESH BUDHATHOKI

A THESIS

**SUBMITTED TO DEPARTMENT OF APPLIED SCIENCE AND CHEMICAL
ENGINEERING PARTIAL FULFILMENT OF THE REQUIREMENT FOR THE
DEGREE OF MASTER OF SCIENCE IN CLIMATE CHANGE AND
DEVELOPMENT**

**DEPARTMENT OF APPLIED SCIENCE AND CHEMICAL ENGINEERING
LALITPUR, NEPAL**

December 2023

COPYRIGHT

The author has agreed that the library, Department of Applied Science and Chemical Engineering, Pulchowk Campus, Institute of Engineering may make this thesis freely available for inspection. Moreover, the author has agreed that permission for extensive copying of this thesis for scholarly purpose may be granted by the professor(s) who supervised the work recorded herein or, in their absence, by the Head of the Department wherein the thesis was done. It is understood that the recognition will be given to the author of this thesis and to the Department of Applied Science and Chemical Engineering, Pulchowk Campus, Institute of Engineering in any use of the material of this thesis. Copying or publication or the other use of this thesis for financial gain without approval of the Department of Applied Science and Chemical Engineering, Pulchowk Campus, Institute of Engineering and author's written permission is prohibited. Request for permission to copy or to make any other use of the material in this thesis in whole or in part should be addressed to:

Head

Department of Applied Science and Chemical Engineering

Pulchowk Campus, Institute of Engineering

Lalitpur, Kathmandu

Nepal

TRIBHUVAN UNIVERSITY
INSTITUTE OF ENGINEERING
PULCHOWK CAMPUS

DEPARTMENT OF APPLIED SCIENCE AND CHEMICAL ENGINEERING

The undersigned certify that they have read, and recommended to the Institute of Engineering for acceptance, a thesis entitled " **Analyzing the Hydrological Regime of Sunkoshi River Basin, Nepal, using a Glacio-hydrological Degree-day Model (GDM)**" submitted by **Sailesh Budhathoki (078MSCCD012)**, in partial fulfillment of the requirements of the degree of **Master of Science (M.Sc.) in Climate Change and Development** Programme.

Supervisor:

MSCCD Coordinator,

.....
Dr. Rijan Bhakta Kayastha

Professor, Department of Environmental
Science and Engineering, School of
Science, Kathmandu University

.....
Dr. Rinita Rajbhandari

Professor, Climate Change and Development
Programme, Department of Applied Science
and Chemical Engineering, IOE, Pulchowk
Campus

Head of Department:

External Examiner:

.....
Dr. Hem Raj Pant

Professor, Department of Applied
Science and Chemical Engineering,
IOE, Pulchowk Campus

.....
Dr. Dhiraj Pradhananga

Associate Professor, Department of
Meteorology, Tri-Chandra Multiple
Campus, Tribhuvan University

Date: December 2023

ABSTRACT

The Glacio-hydrological Degree-day Model (GDM), a distributed and gridded model in glacio-hydrology, uses a temperature index concept to calculate daily river discharge from snow and ice melt, rainfall and base flow. GDM calibration relies on factors like positive degree-days, snow and rain runoff coefficients and recession coefficient. The Sunkoshi River basin is a transboundary river between Nepal and Tibet. The study from 2000 to 2020 A.D includes calibration (2000-2009) and validation (2010-2020) phases in the model simulation. Its robust performance, reflected by Nash-Sutcliffe Efficiency (NSE) values between 0.79 to 0.77, volume difference below 10% and a strong R-squared (R^2) value of 0.83 to 0.77, underscores its reliability. During calibration and validation, snowmelt contributes 9.68% to 11.38%, while clean ice and ice melt beneath debris account for 2.5% to 3% to the total discharge. Rainfall maintains substantial proportions at 48.26% to 50.15%, and baseflow ranges from 37.33% to 37.66% to the total discharge. In May to June's low-flow period, the study shows snow and ice melt greatly affect river discharge. Future analysis predicts a rise in ice melt's influence, especially during low-flow phases, impacting stream flow significantly. However, increasing temperatures reduce snowfall and glacier cover, to the point of diminishing ice and snow melt contributions, ultimately impacting future low-flow stream conditions.

Future peak discharge shifts to July from August with variation in discharge under SSP24.5 and to July with increased discharge post 2030 in SSP58.5 scenarios from the baseline period (2010-2020). Future Projections indicate increased discharge under SSP58.5, notably 3.22 m³/s under EC-Earth3, contrasting with decreases projected under SSP24.5, such as 0.39 m³/s under MPI-ESM1-2HR. SSP24.5 displays baseflow contribution between 32.99% and 34.04%, ice-melt contribution spanning 10% to 13.37%, rainfall contribution fluctuating from 46.51% to 51.13%, and snowmelt contribution ranging from 4.84% to 6.66%. In contrast, SSP58.5 shows a slight uptrend in baseflow (31.62% to 32.07%), substantial increases in ice-melt (14% to 18.12%), stable rainfall (44.56% to 48.8%), and consistent snowmelt (5.13% to 5.71%). Projections for future water scenarios indicate anticipated discharge increases under SSP58.5 and declines under SSP24.5, emphasizing potential resource distribution alterations across different environmental pathways. The GDM emerges as a crucial tool for comprehending hydrological dynamics and evaluating climate change impacts on Himalayan River basins.

ACKNOWLEDGEMENT

I express deep gratitude to my supervisor, Prof. Dr. Rijan Bhakta Kayastha, from the Department of Environmental Science and Engineering at the School of Science, Kathmandu University. His unwavering guidance, wholehearted support, and enthusiastic encouragement have been invaluable. I extend my appreciation to Professor Dr. Rinita Raj bhandari, the Coordinator of the Climate Change and Development Programme at IOE, Pulchowk Campus University, for his valuable insights and unceasing motivation.

Lastly, I wish to convey my heartfelt thanks to my circle of friends and beloved family members for their consistent encouragement and unwavering support whenever I was in need.

TABLE OF CONTENT

COPYRIGHT	2
APPROVAL PAGE	3
ABSTRACT	4
ACKNOWLEDGEMENT	5
TABLE OF CONTENT	6
LIST OF FIGURES	8
LIST OF TABLES	10
LIST OF SYMBOL AND ABBREVIATIONS.....	11
CHAPTER ONE: INTRODUCTION	13
1.1 Background	13
1.2 Statement of the Problem	15
1.3 Research Objectives	16
1.3.1 General Objective	16
1.3.2 Specific Objective	16
1.4 Scope of Study.....	16
1.5 Limitation	17
CHAPTER TWO: LITERATURE REVIEW	18
2.1 Climate change	18
2.2 Climate change in Nepal	18
2.3 Hydrological Model	18
2.4 Glacio-hydrological Model	19
2.5 Modelling approaches	20
2.6 Glacio-Hydrological Degree-day Model (GDM).....	22
2.7 Terms Used in the Model	23
CHAPTER THREE: STUDY AREA AND DATA	29
3.1 Study Area	29
3.2 Input Data	30
3.2.1 Observed Meteorological Data	30
3.2.2 Observed Hydrological Data.....	32
3.2.3 Topographic/Spatial Data	32
3.2.4 Land Use Land Cover Map.....	34
3.3 Bias Corrected Climate Data.....	37

CHAPTER FOUR: RESEARCH METHODOLOGY	39
4.1 Methodological Framework of the Study.....	39
4.2 Estimation of Missing Data.....	40
CHAPTER FIVE: RESULT AND DISCUSSION	43
5.1 Model Calibration and Validation.....	43
5.2 Contribution of Snowmelt, Icemelt, Rain and Baseflow.....	47
5.3 Future Prediction	50
5.3.1 Contribution of streamflow components to the future discharge.....	55
CHAPTER SIX: CONCLUSION AND RECOMMENDATION.....	65
6.1 Conclusion.....	65
6.2 Recommendation.....	66
7. REFERENCES	67

LIST OF FIGURES

Figure 3. 1 Study area map of Sunkoshi River basin, Nepal (up) and the google map of the basin within the red making (image dated: December 31,2020 12:00am) cover the both Nepal and some portion of Tibet (Source: https://earth.google.com/)	30
Figure 3. 2:Hydrological and meteorological station used in Sunkoshi river basin. Dot represents meteorological station whereas the Triangle represents Hydrological station. (Source: https://earth.google.com).....	31
Figure 3. 3:Digital elevation model of Sunkoshi River basin in Nepal.....	33
Figure 3. 4: (a) Land use land cover map of Sunkoshi River basin based on Aster GDEM V3 of 30 m resolution, ESRI Sentinel-2 and Randolph Glacier Inventory (2017),(b) Land use land cover distribution percentage(%) in Sunkoshi River basin,(c) Area-altitude distribution of land use land cover in Sunkoshi River basin based on land use land cover map.	36
Figure 3. 5: Representation of the Quantile-Quantile mapping between model output (x_m) sourced from CMIP6 archive and observed daily maximum temperature x_o across a randomly selected grid-point within the Indian Subcontinent. At 20th percentile ($\phi 0.2$), x_m is lower than x_o for the same quantile, x_m exhibits higher bias than x_o at 60th percentile ($\phi 0.6$). Non-parametric quantile mapping enables the empirical adjustment of model outputs, effectively eliminating systematic bias between x_m and x_o (Mishra et al., 2020).....	38
Figure 4. 1:Flow Chart of Research Methodology	40
Figure 4. 2: Daily maximum temperature between 2000-2020 at the base station i.e. Panchkhal at Sunkoshi river basin.....	42
Figure 4. 3: Daily minimum temperature distribution from 2000 to 2020 at base station i.e. Panchkhal at Sunkoshi River basin.....	42
Figure 4. 4: Observed average precipitation vs observed discharge at outlet of basin i.e. Purchuwarghat (Stn id 630) for the study period from (2000 to 2020) on Sunkoshi River basin.....	43
Figure 5. 1: (A) Precipitation distribution and observed vs Simulated discharge for calibration period (2000-2009) ,(B) Precipitation distribution and observed vs Simulated discharge for validation period (2010-2020), (C) Scatter plots between the observed and simulated values for the calibration period (2000-2009), (D) Scatter plots between the observed and simulated values for the validation periods.(2010-2020).	46
Figure 5. 2: (A) Average monthly discharge contribution graph of baseflow,rain,snowmelt, and icemelt of calibration period (2000-2009). (B) Average monthly discharge contribution graph of baseflow, rain, snowmelt, and icemelt of validation period (2010-2020).	48

Figure 5. 3 (A)Average monthly percentage contribution graph of Snowmelt and Icemelt for calibration period (2000-2009) (B)Average monthly percentage contribution graph of Snowmelt and Icemelt for validation period (2010-2020)49

Figure 5. 4: (A) Future total annual precipitation variation under EC-Earth3 GCM SSP24.5 scenario (2023-2050) (B) Future total annual precipitation variation under EC-Earth3 GCM SSP58.5 scenario (2023-2050) (C) Future total annual precipitation variation under MPI-ESM1-2-HR GCM SSP24.5 scenario (2023-2050) (D) Future total annual precipitation variation under MPI-ESM1-2-HR SSP58.5 scenario (2023-2050) (E) Future total annual precipitation variation under Nor ESM2-MM GCM SSP24.5 scenario (2023-2050) (F) Future total annual precipitation variation under Nor ESM2-MM SSP58.5 scenario (2023-2050).52

Figure 5. 5:(A) Future average annual temperature variation at base station under EC-Earth3 GCM SSP24.5 scenario (2023-2050) (B) Future average annual temperature variation at base station under EC-Earth3 GCM SSP58.5 scenario (2023-2050) (C) Future average annual temperature variation at base station under MPI-ESM1-2-HR GCM SSP24.5 scenario (2023-2050) (D) Future average annual temperature variation at base station under MPI-ESM1-2-HR SSP58.5 scenario (2023-2050) (E) Future average annual temperature variation at base station under Nor ESM2-MM GCM SSP24.5 scenario (2023-2050) (F) Future average annual temperature variation at base station under Nor ESM2-MM SSP58.5 scenario (2023-2050)54

Figure 5. 6:(A) Average annual contribution in future discharge under EC-Earth3 GCM SSP24.5 scenario (2023-2050) (B) Average annual contribution in future discharge under EC-Earth3 GCM SSP58.5 scenario (2023-2050) (C) Average annual contribution in future discharge under MPI-ESM1-2-HR GCM SSP24.5 scenario (2023-2050) (D) Average annual contribution in future discharge under MPI-ESM1-2-HR SSP58.5 scenario (2023-2050) (E) Average annual contribution in future discharge under Nor ESM2-MM GCM SSP24.5 scenario (2023-2050) (F) Average annual contribution in future discharge under Nor ESM2-MM SSP58.5 scenario (2023-2050)58

Figure 5. 7 (A)Average Monthly Contribution graph of Snowmelt and Icemelt under SSP24.5 (2023-2050) (B) Average Monthly Contribution graph of Snowmelt and Icemelt under SSP58.5 (2023-2050).....60

Figure 5. 8:(A) Monthly average simulated discharge during reference time period 2023-2030,2031-2040 and 2041-2050 under SSP24.5(B) Monthly average simulated discharge during reference time period 2023-2030,2031-2040 and 2041-2050 under SSP58.561

Figure 5. 9:(A) Average monthly contribution of hydrological components on discharge in SSP24.5 And SSP58.5 scenarios project by GCM EC-Earth3 for the period (2023-2050) .(B) Average monthly contribution of hydrological components on discharge in SSP24.5 And SSP58.5 scenarios project by GCM MPI-ESM1-2HR for the period (2023-2050) .(C) Average monthly contribution of hydrological components on discharge in SSP24.5 And SSP58.5 scenarios project by GCM Nor ESM2-MM for the period (2023-2050).63

LIST OF TABLES

Table 3. 1:List of Meteorological Stations used in Study	31
Table 3. 2:Hydrological Station used in Sunkoshi river basin	32
Table 5. 1: Calibrated parameters for GDM in Sunkoshi River basin.....	44
Table 5. 2:NSE ,volume difference and R ² of GDM in Sunkoshi River basin.....	46
Table 5. 3 Precipitation and Temperature trend per year up to 2050.....	55
Table 5. 4. Future Discharge trend by 2050 (SSP24.5 and SSP58.5 scenarios).....	59
Table 5. 5. Future Hydrological Component Contributions by 2050 (SSP24.5 and SSP58.5 scenarios).....	59

LIST OF SYMBOL AND ABBREVIATIONS

Apr	April
Aug	August
ASCAT	Advanced Scatterometer
CMIP6	Coupled Model Intercomparison Project Phase 6
CORDEX	Coordinated Regional Downscaling Experiment
Dec	December
DEM	Digital Elevation Model
DHM	Department of Hydrology and Meteorology
E	Easting
ELEV	Elevation
ESRI	Environmental Systems Research Institute
ET	Evapotranspiration
EQM	Empirical Quantile Mapping
Feb	February
GAWSER	Guelph All Weather Sequential Event Runoff
GCM	Global Circulation Model
GDM	Glacio-hydrological Degree-day Model
GHG	Green House Gas
GIS	Geographic Information System
H	Historical
HBV	Hydrologiska Byråns Vattenbalansavdelning model
HEC-HMS	Hydrologic Engineering Center – Hydrologic Modeling
System	
ICIMOD	International Centre for Integrated Mountain Development
IPCC	Intergovernmental Panel on Climate Change
Jan	January
Jun	June
Jul	July

LAT	Latitude
LONG	Longitude
M.a.s.l	Mean above sea level
NASA	National Aeronautics and Space Administration
Nov	November
NSE	Nash-Sutcliffe Efficiency
O	Observed
Oct	October
P	Precipitation
QGIS	Quantum Geographic Information System
RCM	Regional Climate Model
RCP	Representative Concentration Pathway
Sep	September
SRB	Sunkoshi River Basin
SRES	Special Report on Emissions Scenarios
SSP	Shared Socio-economic Pathway
SWAT	Soil and Water Assessment Tool
T	Temperature
UTM	Universal Transverse Mercator
V. D.	Volume Difference
WGS	World Geodetic System
&	Ampersand

CHAPTER ONE: INTRODUCTION

1.1 Background

Our current period is defined by the accelerating pace of global climate change, and the overwhelming consensus among experts is that human actions are the principal cause. According to the Fourth Assessment Report released by the Intergovernmental Panel on Climate Change (IPCC) in 2007, there is a mounting level of confidence that specific extreme weather events will increase in frequency, extent, and severity during the twenty-first century. The rising temperatures and changing climate are exerting a discernible influence on areas with snow and glaciers, resulting in changes to future water supply downstream. The cryosphere, encompassing components like snow, glaciers, permafrost, and ice on lakes and rivers, plays a vital role in high mountain regions, where approximately 10% of the world's population resides. Extensive alterations in the cryosphere have far-reaching consequences on the physical, biological, and human aspects of mountainous areas and the adjacent lowlands. These impacts are discernible even in oceanic environments. (IPCC, 2022). Alterations in snow and glacier conditions have led to shifts in both the volume and timing of runoff within river basins that rely heavily on snow and glacier inputs. These changes have had localized impacts on water resources and agriculture, with a moderate level of confidence in these effects. Notably, there has been an increase in winter runoff in recent decades due to a higher proportion of precipitation falling as rain. Furthermore, in certain river basins fed by glaciers, both summer and annual runoff have increased due to more pronounced glacier melting, while it has decreased in areas where glacier meltwater has reduced due to shrinking glacier coverage. This phenomenon is especially notable in regions dominated by small glaciers, such as the European Alps, with a medium level of confidence. Additionally, glacier retreat and shifts in snow cover have contributed to localized reductions in agricultural yields in specific high mountain regions, including the Hindu Kush Himalaya and the tropical Andes, with a medium level of confidence in these observed impacts (IPCC, 2022).

The Himalayas are distinguished by their numerous glaciers, which serve as a critical, year-round source of water for the rivers that originate from them. Stream are influenced by runoff from precipitation and seasonal snow-ice melting the networks of rivers (Gupta et al., 2019). Assessing the water resources and seasonal and yearly variations in the High Mountain Asia (HMA) area during the last century is of increasing interest to academics across a wide range of disciplines (Kayastha et al., 2020). According to Immerzeel et al.

(2010) The water supply, in the regions of the HMA is especially susceptible, to the impacts of climate change. It heavily relies on snow and glacier melting, which greatly contributes to river flow (Kayastha et al., 2020). Due to the significant contribution of snow and glacier melt to river discharge in the upper sections of the HMA, this area's water supply is particularly vulnerable to climate change (Kayastha et al., 2020).

The energy balance model and the temperature index model are the two melt-modeling techniques now utilized to determine the discharge of river basins that have experienced glaciation. When taking into consideration sums of energy fluxes inside the atmosphere and glacier border, In the energy balance approach the melting process is represented as a residual term, in the equation that describes the energy exchange happening at the surface (Kayastha & Kayastha, 2019). The empirical link between air temperatures and melt rates is what the temperature-index-model, on the other hand, uses to calculate melt (Braithwaite, 1995; Hock, 2003). Even though the energy balance approach (Hock, 2003) provides the assessment of melt totals it may not always be feasible to apply this method to remote Himalayan glaciers due to lack of readily available input data (Kayastha et al., 2020). In research (Kayastha et al., 2000, 2006); (Kayastha & Kayastha, 2019), temperature index models have been employed in Himalayan basins with sparse data to estimate river discharge at various temporal scales. As mentioned by Khadka et al. (2020) the GDM, Version 2.0 is a model that is both distributed and gridded. It has the capability to simulate the impact of elements, on river discharge. Specifically, it considers four runoff components, at intervals; snowmelt, glacier icemelt, rainfall and baseflow (Kayastha et al., 2020). GDM is effective for Himalayan catchments where data scarcity is widespread due to impassable terrain and a dearth of weather stations because it can function with little data and few model parameters (Khadka et al., 2020). The response of rainfall-runoff processes to climate shifts is rapid, whereas glacier melt generation unfolds over longer durations, spanning decades to centuries. This process heavily depends on the available ice volume and the duration under examination. As long as there is sufficient ice, further warming will continue to increase glacier melt. However, a decreasing glacier area will eventually lead to a gradual reduction in melt generation in the long term (Khanal et al., 2021)

1.2 Statement of the Problem

Glaciers and snow-covered areas significantly influence glacierized basin hydrology, with projected climate change expected to alter snow cover and water availability, posing challenges for long-term water management (Khadka et al., 2015). Modelling aids in generating future scenarios for necessary adaptation and mitigation. Over the past three decades, Nepal's total glacier area has decreased by about 25% (ICIMOD, 2014) while diminishing precipitation contributing to snowfall is expected to further increase river flow. Climate change will notably impact rivers in mountainous catchments, necessitating accurate estimation of snow and ice runoff due to the intricate and temperature-dependent nature of the snow melt process.

The CMIP6 model's latest climate projections, presented in Climate Change Assessment Report 6, provide improved projections and higher sensitivity. Despite this, studies on the impact of climate change using the GDM model for SSP scenarios are lacking in this river basin. Glacierized areas often lack comprehensive hydro-meteorological data, affecting model accuracy. Understanding complex glacier dynamics requires considering factors like temperature, topography, and geometry, which can complicate model representation. The interaction between glacier melt and downstream water supply carries socioeconomic implications, warranting the integration of these aspects into the model.

Limited research has been conducted on glacier timing, evolution, and associated runoff changes. A comprehensive study on glacierized basin response to Himalayan climate change is hindered by terrain inaccessibility, sparse climatic data, and non-uniform glacier response across the Himalayas (Kayastha et al., 2020; Khadka et al., 2020). The GDM model fills gaps in previous studies by modeling each component's contribution to stream flow in the Sunkoshi River basin. Several studies like impacts of climate change on hydrological regime and water resource management of Koshi river basin (Devkota & Gyawali, 2015) concludes that temporal variation in river flow is expected to increase in future. Similarly, the study of future climate and its potential impacts on the spatial and temporal hydrological regime in Koshi basin (Bajracharya et al., 2023) states the spatial pattern variability of river discharge. Their limitation was the Weakness of SWAT's snow/glacier component for analysis (Bharati et al., 2019; Pandey et al., 2020) suggest to use other model to simulate snow and glacier. As most of the river of Nepal are glacier fed the contribution of glacier retreat has greater significance.

1.3 Research Objectives

The following are the general and specific objectives of this research:

1.3.1 General Objective

- Analyze the hydrological regime of Sunkoshi River using Glacio-hydrological Degree-day model (GDM)

1.3.2 Specific Objective

- To set up the GDM in Sunkoshi River basin and simulate contribution of hydrological components on stream flow of river.
- Assess the model's ability to simulate stream flow under various climatic scenarios.

1.4 Scope of Study

The specific scope of this study is to conduct research, review, and gather pertinent information from former research articles regarding climate change studies in Nepal. The primary focus is on issues related to water resources, with a particular emphasis on the Sunkoshi River basin. The research aims to examine the impacts of climate change on the hydrology of the Sunkoshi River basin, specifically changes in stream flow. This analysis will be based on the evaluation of hydro-meteorological and spatial data from the catchments of the Sunkoshi River basin, upstream of the watershed outlet.

The study intends to select an appropriate model for watershed modeling, specifically the Glacio-hydrological Degree-day Model (GDM). This model will be chosen based on various available Climate Projection General Circulation Models (GCMs). Suitable projections (CMIP6-GCMs) will be selected for the study area to facilitate future projections. The selected model will be applied to enhance the assessment and prediction of hydrological responses under two scenarios of CMIP6-GCMs climate projections.

The future climatic data derived from CMIP6 will be incorporated into the GDM model to forecast potential consequences in the future. The findings of this research endeavor will provide valuable insights to other researchers engaged in studies concerning climate change, water resources, and hydrology within the power production energy sector.

1.5 Limitation

The study relies significantly on the land use and land cover map of the basin as a primary input for the model. Changes in land use and cover occur over time, including the projected retreat of glacier areas. However, for the model to accurately assess future glacier ice melt contributions, it is crucial to precisely update the changes in glacier coverage within the land use and land cover map. The study encounters a major limitation due to the absence of projected future changes in land use and land cover. While the model undergoes calibration and validation based on simulated and observed discharge, this research overlooks the validation of discharge from individual components such as rain, snowmelt, icemelt, and baseflow. Conducting an Isotope test can effectively scrutinize the roles played by rain, snowmelt, ice melt, and baseflow in the basin's stream flow contribution.

Despite the presence of several meteorological stations in the area, a significant gap in temperature and precipitation data over time restricts the utilization of these station datasets. To mitigate data gap of shorter time frame of used station dataset different interpolation methods were employed. However, these methods might not entirely capture the authentic manifestation of the phenomenon. Moreover, the parameter values used for calibration and validation in the GDM model are derived from various literature reviews of similar river basins rather than actual field-observed values specific to the site. This disparity in values may not necessarily align with the actual physical characteristics of the basin, potentially limiting the accuracy of the study

CHAPTER TWO: LITERATURE REVIEW

2.1 Climate change

It is probable that changes in climate patterns will lead to increased food insecurity due to water scarcity (Wheeler and von Braun, 2013), as well as the potential for reduced access to clean drinking water (Rockström et al., 2012). The difficulties related to water are specific to certain locations and times and can encompass various issues such as the effects of glacier dynamics (Immerzeel et al., 2012), economic and population expansion (Droogers et al., 2012), occurrences of floods, or prolonged periods of drought (Dai, 2011), among other factors. To address these challenges, hydrologists and specialists in water resources are in the process of developing modeling tools. These tools aim to analyze and comprehend the situation and offer potential solutions to aid decision-makers and operational water management (Pechlivanidis et al., 2011).

2.2 Climate change in Nepal

Nepal is contending with the repercussions of climate change, which manifest as rising temperatures, shifts in rainfall patterns, and the gradual disappearance of glaciers. These transformations carry significant implications for Nepal's water resources, agricultural productivity, and ecological balance. According to the sixth assessment report of IPCC, global surface temperature increases contribute to alterations in precipitation patterns, and the warming climate correlates with reductions in snow and ice cover, leading to changes in the cryosphere in high mountain regions. Between 1971 and 2014, Nepal experienced a temperature rise at an annual rate of 0.056°C, with the most substantial warming observed at higher altitudes in the High mountains and Himalayas. Furthermore, there was a decrease in precipitation across all seasons during this period, primarily noticeable in the high Himalayan region (NAP, 2021).

2.3 Hydrological Model

A hydrological model is a mathematical representation of the processes that govern the movement and distribution of water within a specific area or catchment. These models are used to simulate the behavior of the hydrological cycle, which includes processes such as precipitation, evaporation, infiltration, runoff, and streamflow. Hydrological models help researchers, water resource managers, and policymakers understand how water moves through the landscape, predict changes in water availability, and make informed decisions about water management.

2.4 Glacio-hydrological Model

A Glacio-hydrological model serves as a computational aid to understand the intricate interplay between glaciers and the hydrological cycle. Its purpose is to unravel the effects of glaciers on water resources by modeling glacier behavior, such as movement and melting, and how these actions influence streamflow. These models encompass diverse aspects like glacier dynamics, mass balance, meltwater production, runoff generation, and hydrological processes. By incorporating climate data, topographical details, and geometric factors, these models provide valuable insights into the complex relationship between glacier activity and the availability of water resources.

Glacio-hydrological models are constructed from key aspects that work together to simulate the intricate interplay between glaciers and the hydrological cycle:

1. **Glacier Dynamics:** These models encompass algorithms that mimic the motion and deformation of glaciers, capturing how they respond to diverse external factors like temperature shifts and mechanical stress.
2. **Glacier Mass Balance:** By computing the delicate balance between ice accumulation from snowfall and loss due to melting and sublimation, these models unveil the overall health of glaciers, whether they are growing or receding.
3. **Meltwater Generation:** Utilizing inputs such as temperature, solar radiation, and glacier characteristics, the model approximates the magnitude of ice melt—a pivotal factor dictating the extent of glacier-derived runoff.
4. **Runoff Generation:** Glacio-hydrological models portray the interaction between glacier meltwater and other sources of runoff, particularly during periods marked by escalated melting.
5. **Hydrological Processes:** Encompassing a spectrum of phenomena within the hydrological cycle, these processes encompass rainfall, snow accumulation, thawing, evaporation, water infiltration, and the intricate movement of groundwater.
6. **Climate Inputs:** Climate data like temperature and precipitation patterns are essential drivers for these models, steering glacier behavior and the broader hydrological processes.
7. **Topography and Geometry:** The faithful depiction of glacier shape and terrain is of utmost importance, as it underpins a profound comprehension of glacier actions and

their ramifications for local hydrology.

The hydrological modeling landscape encompasses various models serving diverse purposes: The HBV model (Hydrologiska Byrns avdelning for Vattenbalans) adopts a conceptual approach, integrating physical processes and basin structure. It assesses stream flow using temperature and precipitation data, evaluating water balance, flow regimes, and climate change impacts. This model features routines for snow precipitation, soil moisture, and routing, providing continuous discharge simulations at different elevations within the basin.

SPHY (Spatial Processes in Hydrology) is a robust tool designed for cryosphere-hydrological studies. Its SPHY v3 version serves as a spatially distributed water balance model, adaptable across multiple scales, encompassing rainfall-to-runoff transformation, cryosphere processes, evapotranspiration, and soil mechanisms. The JAMS J2000 model (Jena Adaptable Modelling System) employs an open modular approach for preprocessing data and simulating runoff generation. Its modular framework allows for adaptability, eliminating the need for complete model reconstruction.

SWAT (Soil Water Assessment Tool) operates on a daily time step, predicting impacts of management practices on water, sediment, and agricultural yields in vast basins. It doesn't require calibration, relies on available inputs suitable for extensive areas, and operates continuously. HEC-HMS (Hydrologic Modeling System) replicates intricate precipitation-runoff processes within drainage basins. Versatile in deployment across various regions, it tackles challenges from managing water resources in extensive river basins to addressing urban or natural watershed concerns.

The GDM (Glacio-hydrological Degree-day Model) v2.0, a distributed model, simulates daily river discharge, snow melt, ice melt, and rain contributions. It utilizes a temperature index model and is calibrated based on key parameters like positive degree-day factors, snow and rain runoff coefficients, and recession coefficients.

2.5 Modelling approaches

In the realm of contemporary glacier melt modeling, there exist two primary techniques: the energy balance approach and the temperature index model (Kayastha & Kayastha, 2019). These methods find widespread application across various regions worldwide for calculating river basin discharge in areas characterized by glacier coverage. The energy balance approach dissects the process of melting as a residual component within the

equation governing the exchange of energy on the glacier's surface, taking into account a comprehensive summation of energy exchanges involving both the atmosphere and the glacier's boundary (Kayastha et al., 2020). Conversely, the temperature index model relies on empirical relationships between air temperatures and the rate at which melting occurs (Braithwaite, 1995; Hock, 2003). While the energy balance approach excels in accurately estimating the quantity of melt, it encounters limitations when applied to Himalayan glaciers situated in remote areas with limited data availability (Kayastha & Kayastha, 2019).

Melting modeling plays a vital role in any effort to forecast the water runoff from regions covered by snow or glaciers, and also in evaluating transformations in icy regions linked with shifts in climate. Within mountainous terrains, the presence of snow and ice has a notable impact on the hydrology of watersheds, as they store and release water temporarily over different periods (Jansson et al., 2003). Precise measurement of the melting process is critical to the effectiveness of runoff modeling in these kinds of environments. Melt models may be broadly classified into two types: temperature-index models, which assume an empirical link between air temperatures and melt rates, and energy balance models, which try to define melt as residual in the heat balance equation. (Hock, 2003).

The dominant method for melt modeling has been temperature index models, primarily because of four reasons: (1) the extensive accessibility of air temperature data, (2) the relatively uncomplicated methods for estimating and projecting air temperature, (3) the consistent effectiveness of these models despite their basic nature, and (4) their simplicity in computational aspects. Their uses span a wide spectrum, from foreseeing melting for flood forecasts in operational contexts to applications in hydrological modeling (WMO, 1986).

Multiple investigations have brought attention to a robust link between the process of melting and the surrounding air temperature. The study conducted by (Braithwaite & Olesen, 1989) revealed a significant correlation coefficient of 0.96 between the annual reduction of ice and the cumulative positive air temperature. Despite the simplification of intricate processes that are better evaluated through the energy balance of the glacier surface, temperature-index models often achieve performance on a catchment scale comparable to that of energy balance models (WMO, 1986). The efficacy of air temperature as the sole gauge of melt energy, despite the dominance of net radiation as

the energy source for melting, can be attributed to its strong correlation with multiple energy balance components (Braithwaite & Olesen, 1990; Ohmura, 2001) examined the underlying physics of temperature-index models and underscored the role of longwave atmospheric radiation: Typically, this type of radiation functions as the primary heat source for melting and, in combination with sensible heat flux, contributes to roughly 75% of the total energy needed for melting. Both heat fluxes are highly influenced by air temperature, forming the primary basis for the strong connection between melting and air temperature. Additionally, temperature is partially influenced by global radiation (Ohmura, 2001), which functions as a secondary heat source for melting.

2.6 Glacio-Hydrological Degree-day Model (GDM)

According to Kayastha et al.(2020) and Kayastha & Kayastha (2019), GDM, Version 2.0 is a model that is both distributed and gridded. It has the capability to simulate the impact of elements, on river discharge. Specifically, it considers four runoff components, at intervals; snowmelt, glacier ice melt, rainfall and base flow. The basic approach for simulating glacio-hydrological phenomena is carried out by the melt module in GDM utilizing a temperature index model. The calibration of GDM involves adjusting parameters such, as degree day factors, snow and rain runoff coefficients and recession coefficients. These parameters play a role in the calibration process. The values, for degree day factors and critical temperature are determined based on studies (Kayastha et al.,2006 and Khadka et al.,2015). The monthly sunshine hours are required in addition to these factors in order to estimate potential evapotranspiration using the Thornthwaite equation(Gupta et al., 2019). The estimates for potential sunshine hours are based on earlier research (Niroula et al., 2015). Using the degree-day technique, the model independently calculates melt for snow, pure ice, and ice beneath debris. (Khadka et al., 2020) as:

$$M = \begin{cases} (K_d \text{ or } K_s \text{ or } K_b) \times T & \text{if, } T > 0 \\ 0 & \text{if, } T \leq 0 \end{cases} \quad \text{Eq.2.1}$$

The amount of snow or ice melt, in millimeters per day (M) in each grid depends on the air temperature in degrees Celsius (T) well as the degree day factors for snow clean ice and debris covered ice (ks, kb and kd respectively) which represent how much melt occurs per degree Celsius, per day(Khadka et al., 2020), respectively as in Equation. 2.1.

The surface runoff (Q_G) includes the runoff resulting from rainfall melting snow and ice melt, from each grid as indicated in the equation provided below:

$$Q_G = Q_r \times C_r + Q_s \times C_s + Q_i \quad \text{Eq.2.2}$$

In this Equation 2.2, Q_r represents the amount of water flowing from rain Q_s represents the amount of water flowing from melted snow. Q_i represents the amount of water flowing from melted ice all measured in cubic meters, per second (m^3s^{-1}). C_r and C_s are coefficients that represent the impact of rain and snow respectively while Q_G indicates the surface runoff from each grid in $m^3 s^{-1}$. We calculate the contribution of surface runoff (Q_R) from all grids and the total contribution of base flow (Q_B), from all grids. The combined Q_R and Q_B are then directed towards the outlet of the sub basin using a routing Equation 2.3 below:

$$Q_d = Q_R \times (1 - k) + Q_{R(d-1)} \times k + Q_B \quad \text{Eq.2.3}$$

The recession coefficient, represented by the variable "k " is used to calculate the total discharge denoted as " Q_d " in cubic meters per second for a given day ("d"). To determine the value of "k " we solve Equation 2.4. The constants "x" and "y," obtained from this equation are computed as 0.93 and 0.009 for the basin.(Khadka et al., 2020)

$$k_{d+1} = x Q^{-y}_d. \quad \text{Eq.2.4}$$

2.7 Terms Used in the Model

Different terms that are used in the model are depicted below.

Grid:	Number of grids in which the study basin is divided
Reference Station Elevation:	Base station elevation for temperature (T) and precipitation (P) in m a.s.l.
Lower/Higher Elevation:	Lower elevation (LE) is usually the elevation from where glacier starts.
Higher elevation (HE):	Elevation from where the degree day factors need to be changed. These LE and HE are used to assign different degree-day factors for the basin.
Debris-covered glacier area:	Area of the basin covered by debris-covered glacier (km^2) (If the basin does not has debris-covered glacier ice, then the debris-covered glacier area at each zone = 0)
Clean glacier area	Area of the basin covered by a clean glacier (km^2)
k:	Degree-day factor ($mm/^\circ C/d$); k_s and k_b refer to degree-day factors for snowmelt and icemelt,

	<p>respectively. These values may differ according to the elevation of the basin, which is denoted by LE and HE for lower elevation and higher elevation, respectively.</p> <ul style="list-style-type: none"> • k [LE] represents the degree-day factors for the elevation zones that starts from the lower elevation to zone below higher elevation defined by the user. • k [HE] represents the degree-day factors for the elevation zones that start from the higher elevation defined by the user.
Cr and Cs:	<p>Cr and Cs: Runoff coefficient expressing losses as a ratio of the measured precipitation to the measured runoff, where Cr and Cs refer to rain coefficient and snowmelt runoff coefficients, respectively. The program accepts different values of Cr and Cs for different months.</p>
Critical Temperature:	<p>Critical temperature ($^{\circ}\text{C}$) determines whether the measured precipitation is rain or snow at that temperature</p>
Temperature lapse rate:	<p>Temperature lapse rate ($^{\circ}\text{C}/100\text{ m}$) can be obtained from the temperature stations available at different elevations within the basin or from nearby stations that can represent the climatic condition of the basin. The program accepts different temperature lapse rate values for different zones.</p>
x and y:	<p>x and y are the constants used to calculate the recession coefficient (k)</p>

Model Accuracy:	<p>The model accuracy can be assessed through two accuracy criteria:</p> <p>(i.) Nash – Sutcliffe Coefficient (da Silva et al., 2015; Nash & Sutcliffe, 1970)</p> $NSE = 1 - \frac{\sum_{i=1}^n (Q_i - Q'_i)^2}{\sum_{i=1}^n (Q_i - \bar{Q})^2}$ <p>Where</p> <p>n: Number of days</p> <p>Q_i: Daily measured discharge</p> <p>Q'_i: Simulated measured discharge</p> <p>\bar{Q}: Average discharge of the given year in m³/s.</p>
	<p>(ii.) Volume Difference (Khadka et al., 2020):</p> $VD(\%) = \frac{V_R - V'_R}{V_R} \times 100$ <p>Where V_R: Measured runoff volume</p> <p>V'_R: Simulated runoff volume in m³.</p>

GDM is temperature index models have been employed in Himalayan basins with sparse data to estimate river discharge at various temporal scales. Multi –model assessment of Glacio hydrological change in central Karakoram, Pakistan by (Hassan et al., 2021) GDM simulated river discharge with the improved accuracy of 0.87 for the calibration and 0.84 NSE for the validation period. The comparative study of hydrology and ice melt in three river basin of Nepal Trishuli, Tamor and Marsyangdi river basin using GDM estimated contribution of snowmelt, ice melt, rainfall and base flow to be most accurate in Trishuli river basin with Nash-Sutcliffe efficiency (NSE) between the estimated and observed discharge of 0.81 and volume difference of -0.5%. (Kayastha et al., 2020). Use of GDM to estimate discharge from glacierized Himalayan river basins for both the calibration and validation period NSE value are between 0.76 and 0.83 and R² 0.8 which is very promising result for Trishuli and Marsyangdi River basin (Kayastha & Kayastha, 2019). Sensitivity analysis of model performance results that output of GDM are highly Sensitive to variation in temperature than variation in precipitation (Hassan et al., 2021). According to a study conducted on Koshi basin by Khadka et al. (2020) it is predicted that

the average area covered by glaciers, in all sub basins will decrease significantly between 2021 and 2100. Similarly, the study forecasts a decrease of 76 and 86% in the volume of glaciers for RCP 4.5 and 8.5 scenarios respectively. Looking ahead to beyond 2060 the study suggests that there will be an increase in discharge, during the pre monsoon seasons while a decrease can be expected during the post monsoon and winter seasons. This projection may ultimately lead to seasons and drier dry seasons (Khadka et al.,2020). For the study minimum one metrological station and one hydrological station is required. Those station are marked as reference stations The research utilizes the temperature and precipitation data collected from reference stations on a basin. This data is then fed into a GDM model to estimate the temperature lapse rate and precipitation gradient using information, from stations. Afterwards the temperature and precipitation values are allocated to each grid based on the temperature lapse rate observed at the reference stations(Khadka et al.,2020).The GDM has been effectively applied in three glacierized river basins in Nepal: Tamor, Trishuli, and Marsyangdi. The computed discharges generated by the GDM align closely with the observed discharges from the respective rivers. The Nash-Sutcliffe Efficiency (NSE) values range from 0.69 to 0.81, and the volume differences fall within the range of -7.51% to 4.64% (Kayastha et al., 2020). Among these basins, the Trishuli River exhibits the highest snowmelt contribution to river flow, accounting for 13.93% of the total, while the Marsyangdi River basin demonstrates the lowest snowmelt contribution at 7.8%. In the case of ice melt contribution, the Marsyangdi River basin records the highest value of 12.88%, whereas the Tamor River basin displays the lowest ice melt contribution at 6.6%. It is noteworthy that the variations in maximum and minimum ice melt contributions within the Marsyangdi and Tamor River basins, respectively, correspond to the varying extents of permanent ice cover in these basins. This consistency highlights the connection between ice melt contribution and the extent of permanent ice cover in these specific regions. (Kayastha et al., 2020). The study on a multimodel assessment of glacio-hydrological changes in the central Karakoram region of Pakistan. The investigation employs two models, namely the Modified Positive Degree-day Model (MPDDM) and the Glacio-hydrological Degree - day Model (GDM), within the Shigar River basin. The findings from both models underscore the significance of snow and ice melt in maintaining river flow within the catchment.

Notably, the MPDDM suggests that despite relatively low precipitation during the

summer monsoon, rain and base flow still contribute significantly to the annual river runoff, accounting for 68%. In contrast, the GDM attributes a smaller contribution of 14% to rain and base flow. Similarly, the MPDDM and GDM diverge in estimating the annual stream discharge derived from snow and ice melt, with values of 32% and 86%, respectively (Hassan et al., 2021). For the simulation of river discharge, the MPDDM achieves Nash-Sutcliffe Efficiency (NSE) values of 0.86 and 0.78 during calibration and validation, respectively. In parallel, the GDM demonstrates improved accuracy, yielding NSE values of 0.87 and 0.84 during the calibration and validation periods, respectively (Hassan et al., 2021). The GDM showed accuracy in simulating the daily river runoff compared to the MPDDM when compared to the observed river discharge. The model successfully replicated both peak flows aligning with the measured values although it overestimated river discharge in April and March. Throughout the winter season the river discharge remained stable at an average of $21 \text{ m}^3 \text{ s}^{-1}$ in January. As temperatures rose the discharge gradually increased due, to snowmelt (Hassan et al., 2021).

The utilization of OGEM and GDM in projecting streamflow alterations within the Urumqi river head watershed in the Tianshan Mountain region, China, demonstrated the GDM's greater sensitivity to shifts in air temperature than changes in glacier extent, as evidenced by (Yang et al., 2022). Under all SSP scenarios, the anticipated reduction in projected runoff signaled the passage of peak runoff timing. The research indicated that a 2°C rise in monthly average temperature could result in a substantial 37.7% surge in the total basin discharge (Yang et al., 2022). The model's calibration employed five years of data (2007-2011), followed by seven years of data (2012-2018) for validation. It was considered that the model was accurate and dependable if NSE exceeded 0.7 and V.D remained within a 10% range, following the criteria established by (Khadka et al., 2020). However, it should be noted that the model's representation of runoff is less effective during periods of high precipitation events, generally speaking, the GDM effectively elucidates the hydrological processes within the Urumqi River basin's head watershed.

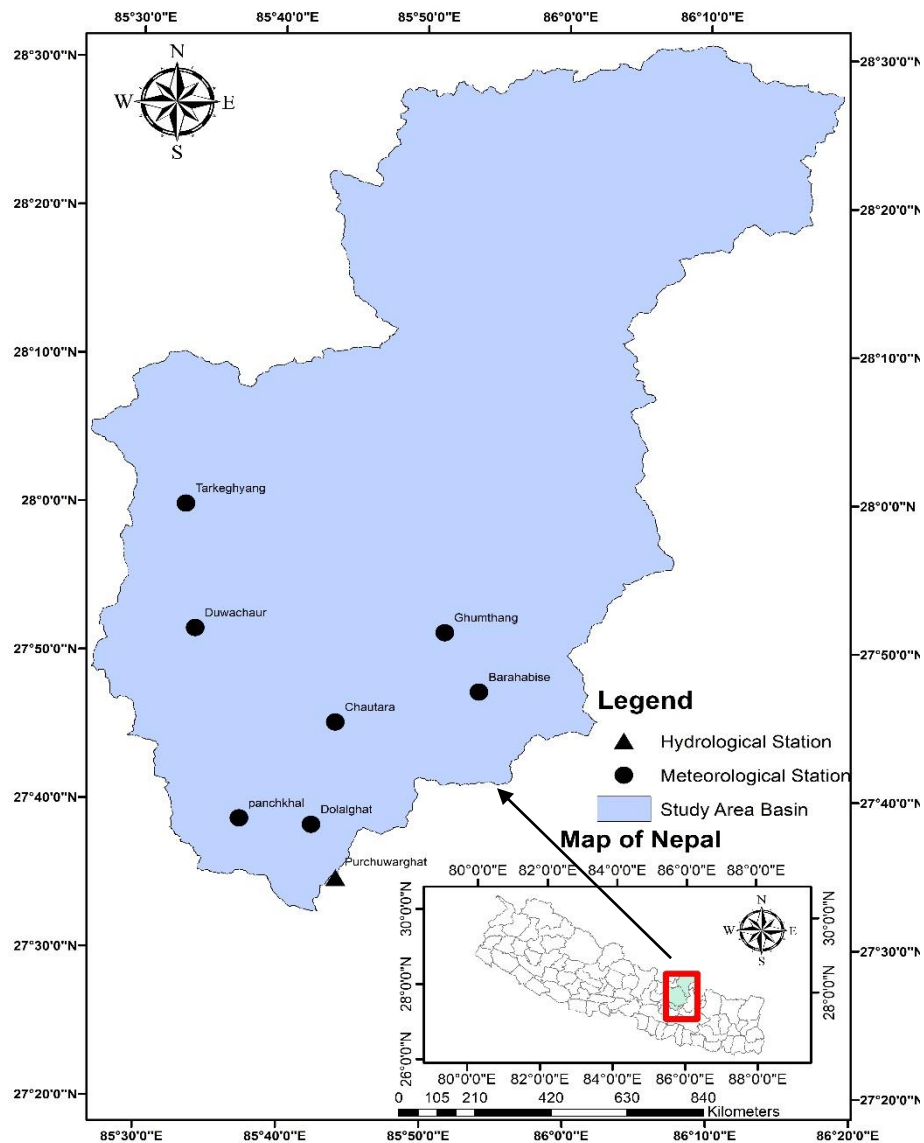
Numerous research has applied hydrologic models for the assessment of prospective effects of climate change on water resources. (Githui et al., 2009) used soil and water assessment tool (SWAT) model to investigate the impact of climate change on streamflow in western Kenya. (Roy et al., 2001) used a coupled hydrology-hydraulics model of the basin to examine the effects of climate change on summer and fall flooding in a southern Quebec basin, Canada. Similarly, (Shrestha et al., 2016) used SWAT model

for modelling the potential impacts of climate change on hydrology and water resource in river basin and similarly impacts of climate change on hydrological regime and water resource management of Koshi river basin (Devkota & Gyawali, 2015). Their findings suggested that average annual precipitation in the basin is projected to increase in time with the spatial and temporal variation and on different future climate scenarios. Most of the study on river discharge has been done using Soil and Water Assessment Tool (SWAT). The model has not been calibrated specifically for replicating catchments even though it performs all its estimations at a very small geographical scale. Moreover, when compared to the rainfall runoff aspect, the snow/glacier component of SWAT's relatively weaker (Bharati et al., 2019; Pandey et al., 2020). Therefore, if these factors are significant and require, in depth analysis it is recommended to consider using snow/glacier models (Adnan et al., 2019). So to overcome the limitation of SWAT, many researcher has been using Glacio-hydrological Degree-day model (GDM).

CHAPTER THREE: STUDY AREA AND DATA

3.1 Study Area

Between Tibet (China) and Nepal, there is a transboundary river basin known as the Sunkoshi. It spans between 27° 30' to 28° 32' Northing and 85° 28' to 86° 20' Easting, on northern hemisphere with an altitude range of 578 to 7945 m above sea level (Figure 3.1). The basin has a surface area of about 4798.05 km², of which 2791.05 km² are in Nepal and about 2007 km² are in Tibet. This basin has nine lakes, all of which are in Tibet, that may be harmful. Lumi Chimi lake, located at (28° 19' N and 85° 51' E), is among the most hazardous. The lake is located at an elevation of 5089 m above sea level (Shrestha et al., 2010). In Tibet, the river flows out of the Lumi Chimi and drains into the Poiqu river. After entering the territory of Nepal the river is called Bhotekoshi. Further, this river meets the Sunkoshi river near the town Bahrabise, where it takes the name of Sunkoshi. (Shrestha et al., 2010)



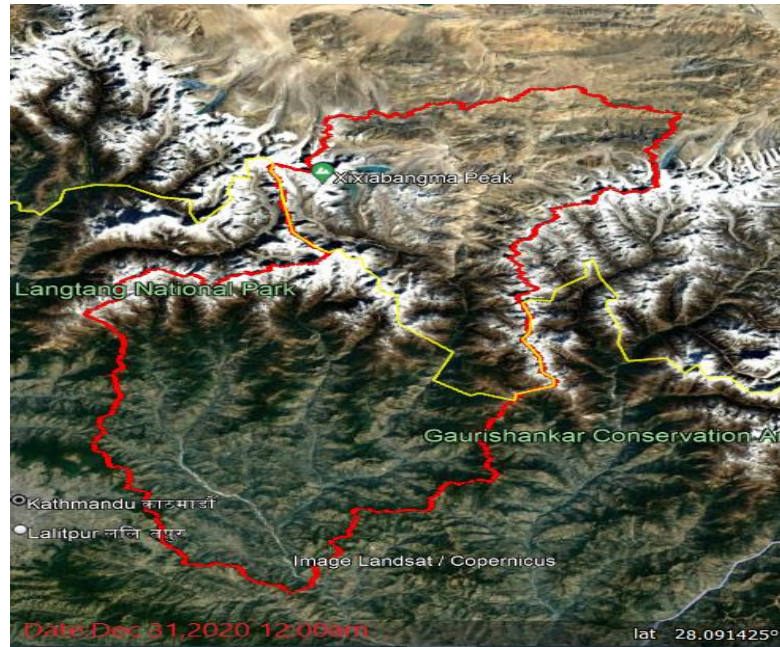


Figure 3. 1 Study area map of Sunkoshi River basin, Nepal (up) and the google map of the basin within the red making (image dated: December 31,2020 12:00am) cover the both Nepal and some portion of Tibet (Source: <https://earth.google.com/>)

3.2 Input Data

3.2.1 Observed Meteorological Data

Hydrological and meteorological daily observed data set of air temperature, precipitation and streamflow data are obtained from Department of Hydrology and Meteorology (DHM), Government of Nepal. The hydrological meteorological stations in the basin is also shown in Figure 3. 2. According to the data records of the DHM, there are a total of 282 operational meteorological stations throughout Nepal. Among these, fifteen stations are located in the vicinity of the Sunkoshi Basin. The daily observed average precipitation for Station No. Tarkeghyang (1058), Panchkhal (1036), Duwachaur (1017), Dolalghat (1023), Bahrabise (1027), and Ghumthang (1006) was collected from the Department of Hydrology and Meteorology (DHM) for the baseline period of 2000 to 2010 to estimate the average basin precipitation. Out of the 15 meteorological stations, six stations were selected for the study, and 3daily meteorological data were obtained. The remaining nine stations had significant gaps in observations compared to the selected six stations. The list of meteorological stations used in this study is provided in Table 3.1.

Similarly, there are five temperature stations within the Sunkoshi basin, namely Madan (1020), Sermathan (1016), Panchkhal (1036), Bahrabise (1027), and Chautara (1009). However, we have only considered temperature data from the Panchkhal station. This

decision was made because the other two stations have a substantial amount of missing data, while the Panchkhal Station provides more reliable temperature data for the study basin.

For precipitation data, we have collected data for the basin spanning 20 years, from 2000 to 2020. It would have been more significant if the available data range exceeded 50 years for each station. Similarly, for temperature data, we have a 20-year dataset covering the period from 2000 to 2020. To facilitate model calibration and validation, we have utilized weather data from the years 2000 to 2009 for calibration and 2010 to 2020 for validation, spanning a total of 20 years, ensuring consistency in the study period.

Table 3. 1:List of Meteorological Stations used in Study

S. no	Station ID	Name	District	Latitude	Longitude	Elevation
1	1009	Chautara	Sindhupalchowk	27.75	85.73	1552
2	1006	Ghumthang	Sindhupalchowk	27.86	85.86	1885
3	1017	Duwachaur	Sindhupalchowk	27.85	85.56	1481
4	1023	Dolalghat	Kavrepalanchok	27.63	85.70	659
5	1027	Bahrabise	Sindhupalchowk	27.78	85.89	884
6	1036	Panchkhal	Kavrepalanchok	27.64	85.62	857
7	1058	Tarkeghyang	Sindhupalchowk	27.99	85.55	2596

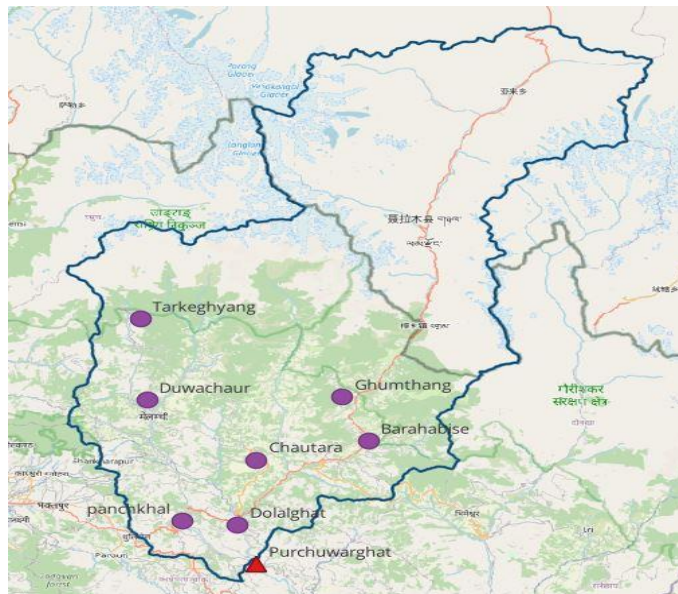


Figure 3. 2:Hydrological and meteorological station used in Sunkoshi river basin. Dot represents meteorological station whereas the Triangle represents Hydrological station.

(Source:<https://earth.google.com>)

3.2.2 Observed Hydrological Data

There are a total of 51 hydrological stations located across the country, with four stations, namely Purchuwarghat (630), Dolalghat (629.1), Bhotekoshi (Station no. 610), and Balephi (Station no. 620), situated within the basin. The Purchuwarghat hydrological station (Station no. 630) was selected as the outlet point for the study. Daily observed data obtained from DHM were available for the period 1964 to 2020 for the Purchuwarghat station.

The study utilized daily observed data from the years 2000 to 2020. The gauged flow data were incorporated into the model for two key purposes: firstly, to establish inlet discharge points for simulating the existing conditions within the basin, and secondly, for conducting sensitivity analysis, calibration, and validation of the model at the outlet. The calibration process utilized daily observed data spanning 2000 to 2010 AD, while the validation phase employed data from 2011 to 2020 AD. Detailed overview of the gauging stations is presented in Table 3.2.

Table 3. 2:Hydrological Station used in Sunkoshi river basin

S. no	Station ID	Name	District	Latitude	Longitude
1	630	Purchuwarghat	Kavrepalanchok	27° 33' 30''	85° 45' 10''
2	629.1	Dolalghat	Kavrepalanchok	27° 38' 20''	85° 42' 30''
3	610	Bhotekoshi	Sindhupalchowk	27° 47' 10''	85° 53' 20''

3.2.3 Topographic/Spatial Data

The topography of this research area was determined using a digital elevation model with a resolution of 30 meters available in GeoTIFF file format. Grid elevation data in GDM is calculated using the Advanced Space borne Thermal Emission and Reflection Radiometer (ASTER) Global Digital Elevation Model (GDEM) v3, with a resolution of 30 meters, available from the Earthdata (<https://www.earthdata.nasa.gov/>). Figure 3.3 illustrates the digital elevation model of the study area. Sinks and pits that could inadvertently trap water in the terrain are corrected by adjusting the elevation of the pit cells to match that of the surrounding cells. Topographical information is extracted from the DEM for the basin. Using QGIS, downloaded data was projected to WGS 1984 UTM Zone 45N and then

clipped to create the DEM of the research region. The DEM was employed in GIS to delineate the watershed and derive the river network, drainage pattern, slope length, gradient, sub-basin, and other terrain-related details. The DEM file, processed through GIS operations, serves as the initial input data for running the GDM model. Elevation values range from 578m to 7945m.

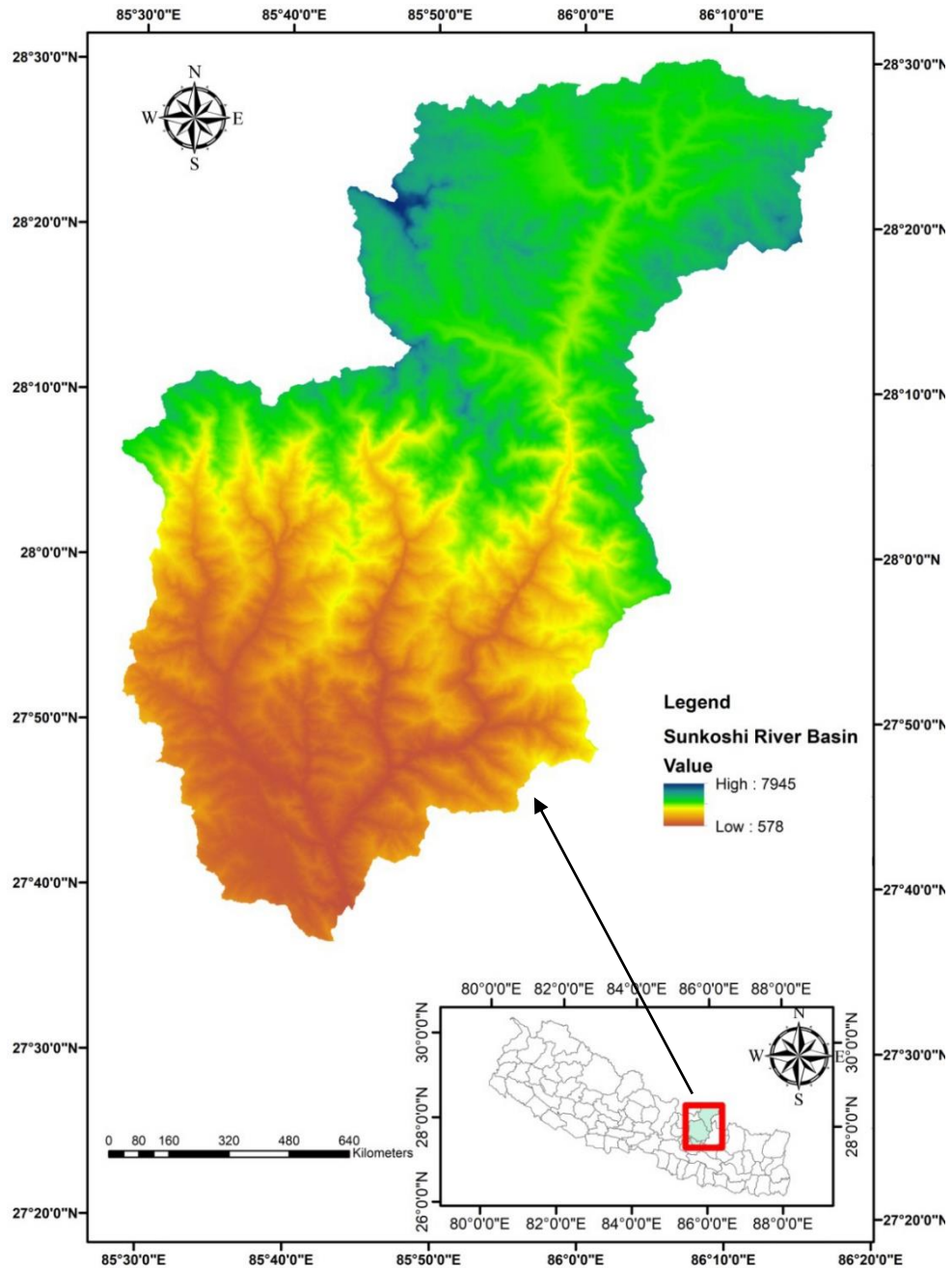


Figure 3. 3: Digital elevation model of Sunkoshi River basin in Nepal

3.2.4 Land Use Land Cover Map

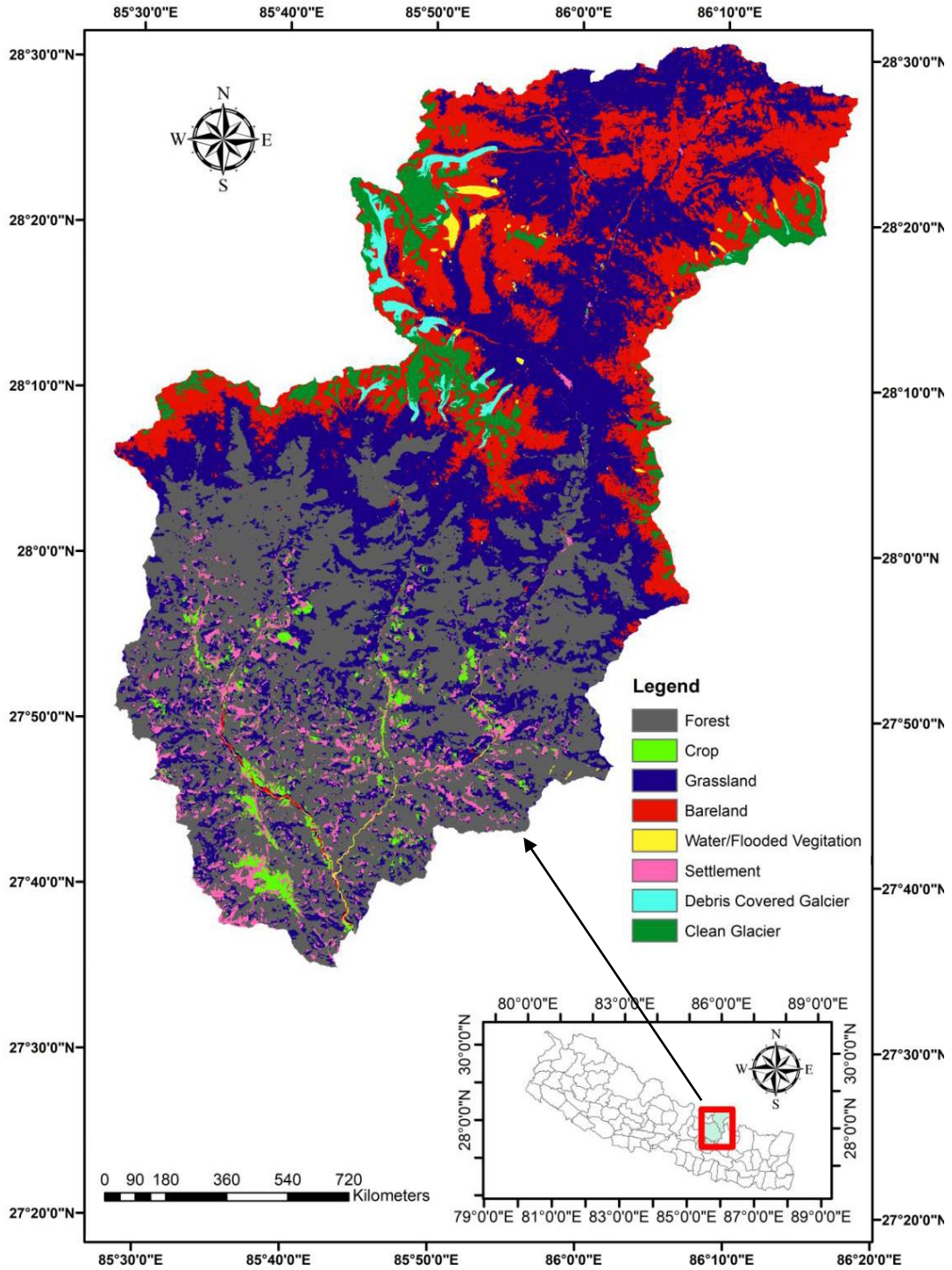
Global land use/land cover data of 10 m resolution from Sentinel-2 was acquired from ESRI. The inventory of clean and debris-covered ice glaciers was sourced from the RGI Consortium (2017). The dataset, titled "Randolph Glacier Inventory - A Dataset of Global Glacier Outlines, Version 6," is available in the form of a shape file [Data Set]. It was published by the National Snow and Ice Data Center in Boulder, Colorado, USA, and can be accessed at <https://doi.org/10.7265/4m1f-gd79>.

To create the comprehensive map required by the GDM model, the shape file containing information about clean and debris-covered ice was projected onto the global land use/land cover data from Sentinel-2. Land cover Map consisting of eight land classes for the Sunkoshi River basin shown in Figure 3.4. Land use land cover is classified into 8 Classes:

- i. Forest
- ii. Crops
- iii. Grassland
- iv. Bareland
- v. Wetland
- vi. Settlement
- vii. Debris Covered Glacier
- viii. Clean Glacier

The land use pattern of the study area has been given in figure below. The components included in the Sunkoshi River basin are forest (33.00%), crops (1.00%), grassland (37.00%), barelands (19.00%), wetlands (1.00%), settlements (4.00%), debris covered glaciers (1.00%) and clean glaciers (4.00%). In the study area, eight different land use types are preserved. The majority of the area is covered by grass land and forest, followed by forest. bareland, crops, and built-up areas cover a smaller area than other types.

a.



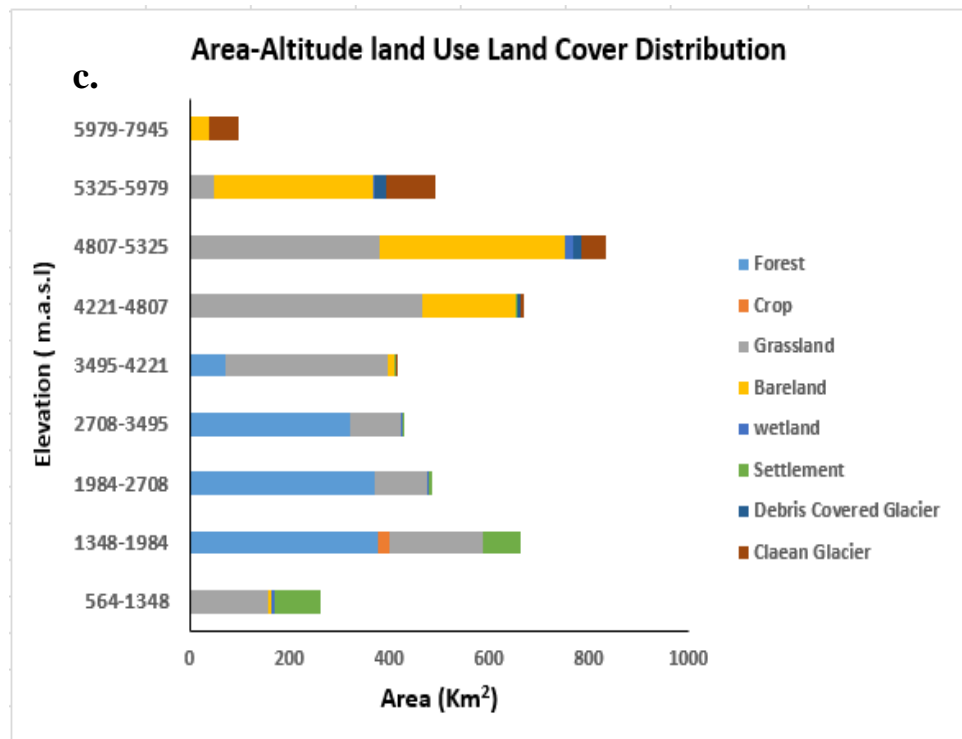
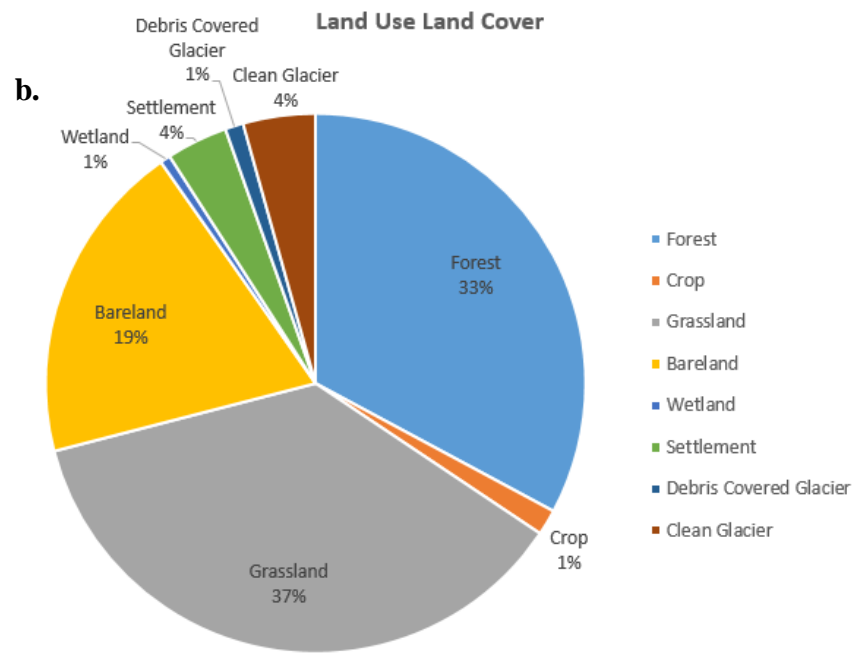


Figure 3. 4: (a) Land use land cover map of Sunkoshi River basin based on Aster GDEM V3 of 30 m resolution, ESRI Sentinel-2 and Randolph Glacier Inventory (2017),(b) Land use land cover distribution percentage(%) in Sunkoshi River basin,(c) Area-altitude distribution of land use land cover in Sunkoshi River basin based on land use land cover map.

3.3 Bias Corrected Climate Data

The imminent threat of climate change is poised to bring forth significant challenges across various sectors in South Asia, including agriculture, water resources, infrastructure, and the livelihoods of millions. To address this challenge, comprehensive dataset that includes daily bias-corrected records of vital variables like precipitation, maximum and minimum temperatures. The dataset, with a spatial resolution of 0.25° , covers an expansive area that includes countries such as India, Pakistan, Bangladesh, Nepal, Bhutan, and Sri Lanka. Furthermore, it encompasses 18 river basins nested within the broader Indian subcontinent (Mishra et al., 2020). The development of bias-corrected dataset relies on the skillful application of Empirical Quantile Mapping (EQM) techniques. It serves as a historical record, spanning from 1951 to 2014, while also providing future projections from 2015 to 2100 under four distinct scenarios (SSP126, SSP245, SSP370, and SSP585) using data from 13 General Circulation Models (GCMs) sourced from the Coupled Model Intercomparison Project-6 (CMIP6). The rigorous validation process for this bias-corrected dataset involves a comprehensive examination against observed data, covering both average and extreme precipitation, as well as maximum and minimum temperatures. For bias correction (Figure 3.5), statistical transformations are employed to discover a function that links the model's output to a fresh distribution, aligning it with the distribution seen in the actual observations. Typically, this transformation can be expressed mathematically (Piani et al., 2010) as Equation.3.1:

$$x_m^o = f(x_m) \quad \text{Eq.3.1}$$

where x_m^o is the bias-corrected model output. If the statistical distribution of x_m and x_o are known, the transformation can be written as Equation.3.2:

$$x_m^o = F_0^{-1}(F_m(x_m)) \quad \text{Eq.3.2}$$

The resulting bias-corrected projections from 13 CMIP6-GCMs offer a detailed view of South Asia's path towards a warmer ($3\text{--}5^\circ\text{C}$) and more moisture-rich (13–30%) climate throughout the 21st century. These projections, meticulously fine-tuned through the lens of bias correction, are ready to support precise assessments of climate change impacts in South Asia and serve as a cornerstone for hydrological impact evaluations within the complex network of subcontinental river basins. It's important to note that this dataset has been statistically downscaled and bias-corrected using Empirical Quantile Mapping (Mishra et al., 2020)

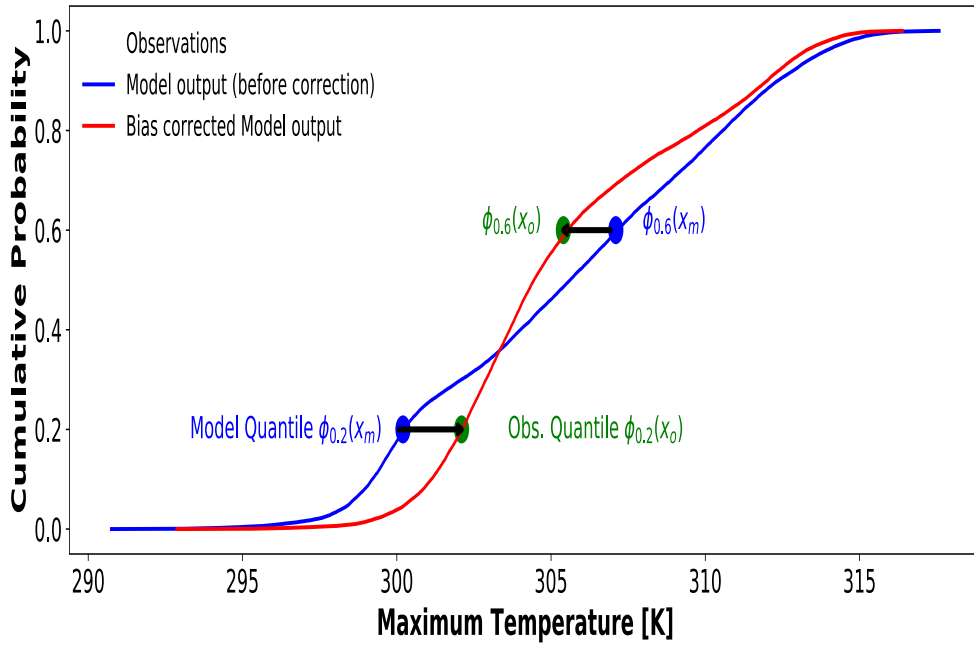


Figure 3. 5: Representation of the Quantile-Quantile mapping between model output (x_m) sourced from CMIP6 archive and observed daily maximum temperature(x_o) across a randomly selected grid-point within the Indian Subcontinent. At 20th percentile ($\phi_{0.2}$), x_m is lower than x_o for the same quantile, x_m exhibits higher bias than x_o at 60th percentile ($\phi_{0.6}$). Non-parametric quantile mapping enables the empirical adjustment of model outputs, effectively eliminating systematic bias between x_m and x_o (Mishra et al., 2020)

Among 13 different biased corrected GCMs data available, three GCMs (EC-Earth3, MPI-ESM1-2-HR, Nor ES2-MM) with higher resolution were chosen and used as the input to the GDM to simulate future discharge and its contributors under SSP24.5 and SSP58.5 climate scenarios from 2023 to 2050. In glacierized catchments a warm and dry situation is considered a scenario. The purpose of this study is to examine the glacio conditions that may occur under this extreme projection.

CHAPTER FOUR: RESEARCH METHODOLOGY

4.1 Methodological Framework of the Study

The model's discharge simulation is driven by daily extrapolated temperature and precipitation data, which are extended from the reference station to each grid. The distinction between snow and rain within each grid and time step is determined by the threshold temperature (T_T) (Kayastha & Kayastha, 2019) as follows:

$$\text{Precipitation} = \begin{cases} \text{rain, if } T \geq T_T \\ \text{Snow, if } T < T_T \end{cases}$$

Where T represents the extrapolated daily air temperature for the grids, and T_T signifies the threshold temperature, both measured in degrees Celsius. In each grid, the calculation of daily ice melt from debris-free and debris-covered ice, along with snow melt from glacierized and glacier-free areas (Khadka et al., 2020), is as follows:

$$M = \begin{cases} (K_d \text{ or } K_s \text{ or } K_b) \times T & \text{if } T > 0 \\ 0 & \text{if } T \leq 0 \end{cases}$$

Here, M denotes the ice or snow melt in millimeters per day (mm/day) within each grid, while T represents the daily air temperature in degrees Celsius ($^{\circ}\text{C}$). The parameters K_d , K_s , and K_b stand for the degree-day factors associated with ice under debris, snow, and clean glacier ice, respectively, measured in millimeters per degree Celsius per day ($\text{mm } ^{\circ}\text{C}^{-1} \text{ day}^{-1}$) (Khadka et al., 2020). The model accounts for the multilayer melting of snow over both clean ice and debris-covered ice.

For base flow calculation, a simulation approach similar to SWAT is employed. This involves utilizing a two-aquifer system concept—shallow and deep aquifer systems—to simulate base flow in a basin dominated by glacier and snow melt (Luo et al., 2012; Y. Zhang et al., 2015). The advantage of employing a two-reservoir system over a single-reservoir system lies in its ability to release discharge during the recession period, ensuring a closer alignment between simulated and observed discharge levels. Figure 4.1. illustrates the overall framework that were carried out to analyze and evaluate the model performance in simulating the discharge and present the contribution of different streamflow components for this study.

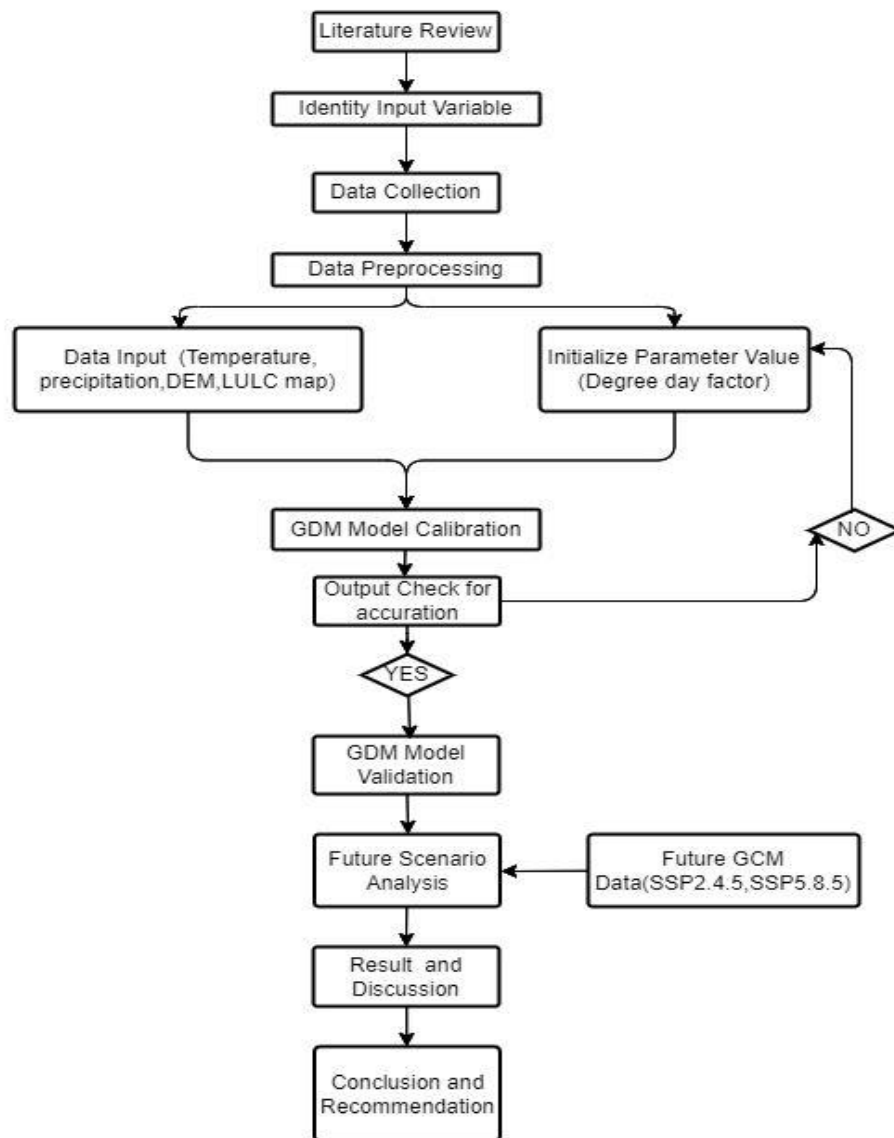


Figure 4. 1:Flow Chart of Research Methodology.

4.2 Estimation of Missing Data

Hydro-meteorological data is an important part of the hydrological modelling and simulations. Obtaining trustworthy data is one of the first tasks in every hydrological and meteorological investigation (Sattari et al., 2017). The weather data required as input to the model are precipitation, temperature. The data available from DHM, Nepal had a lot of missing data. The missing data in some cases were even to the extent that month-long gaps were noticed. All these data from respective gauge stations lying at the vicinity or inside the basin are fed into the GDM for continuous event simulations. The hydrological simulation is performed using the observed data available from 2000-2020. IDW was selected for this investigation in order to estimate and fill in the gaps left by missing daily

rainfall data. Data from the closest source that provided accessible data on the same days were used to estimate the missing values

i. Inverse Distance Weighting Method (IDW)

The IDW approach is predicated on how close the target station (TS) is to nearby stations (SSs). The weighted component in this technique was the distance between the TS and SSs, which was calculated as follows.:

$$W_i = \frac{d_i^{-n}}{\sum_{i=1}^m d_i^{-n}}$$

where m is the total number of SSs in operation and d_i is the distance between TS and SSs. The value of power "n" typically falls within the range of 1 to 6. However in this study we also use the employed value of 2 (Barrios et al., 2018; Teegavarapu & Chandramouli, 2005). As the distance, between the stations increases the weight assigned by Inverse Distance Weighting (IDW) decreases. When stations are apart each station gives importance to readings from nearby stations.

ii. Temperature Lapse Rate Method (TLR)

Temperature data from the Panchkhal, Chautara, and Bahrabise stations within the Sunkoshi River Basin were collected, encompassing the period between 1990 and 2022. Missing temperature data at each station posed a challenge, and to address this, the temperature lapse rate method was employed. This method becomes particularly valuable in high-altitude regions with limited or no station data, such as glacier and snow-covered watersheds (Zhang et al., 2018) In these contexts, the lapse rate method is utilized for estimating missing temperature data, enhancing the efficiency of observed and predicted stream flows.

The lapse rate, defined as the temperature decline with increasing altitude, was determined by calculating the station-to-station lapse. Interpolation of missing data relied on the lower elevation station's data. The essential equation for estimating temperature data is:

$$Lr = (T2 - T1) / (E2 - E1)$$

Where: T1 and T2 are the mean temperatures of the stations; E1 and E2 are the elevations of the stations; Lr is the lapse rate for the considered stations.

The missing temperature data for each station were determined using the following equation, leveraging the station's lapse rate:

$$T2 = T1 + Lr * T1$$

Here: T1 represents the known temperature data of the station, T2 stands for the missing temperature data of the station.

This study estimated missing temperature data for all stations using the aforementioned lapse rate equations

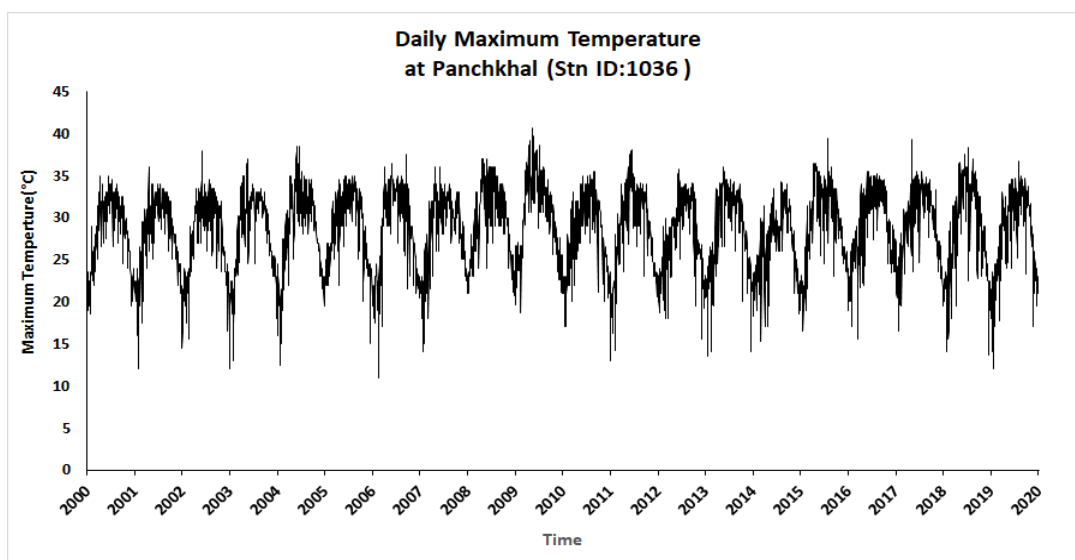


Figure 4. 2: Daily maximum temperature between 2000-2020 at the base station i.e. Panchkhal at Sunkoshi River basin

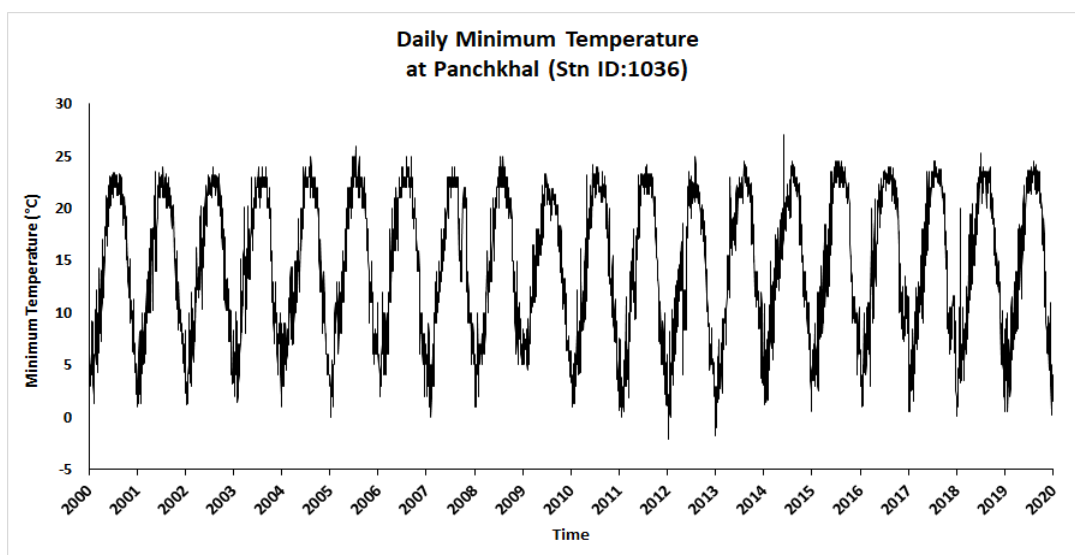


Figure 4. 3: Daily minimum temperature distribution from 2000 to 2020 at base station i.e. Panchkhal at Sunkoshi River basin

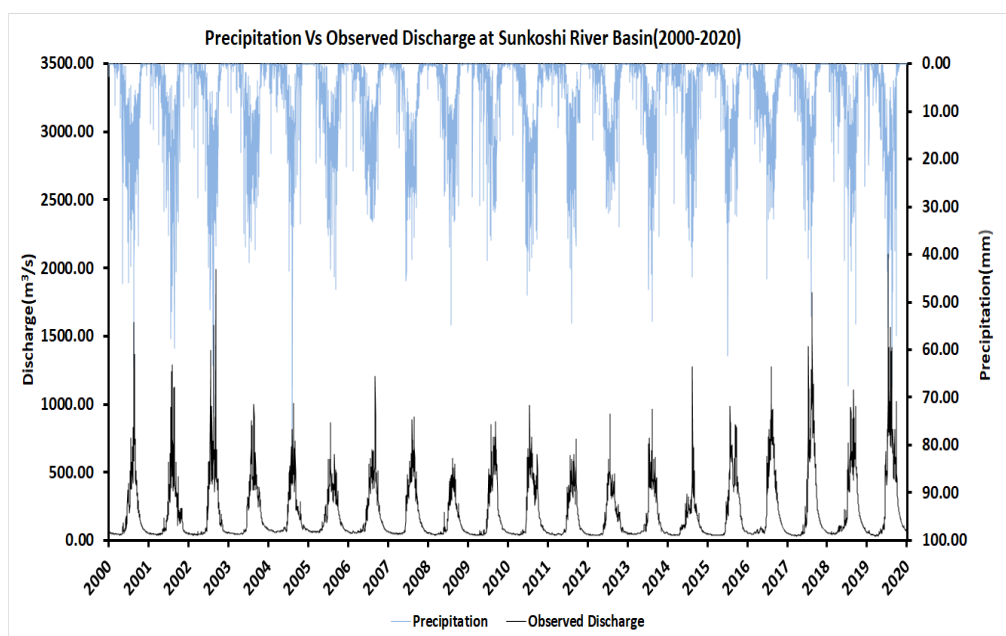


Figure 4. 4: Observed average precipitation vs observed discharge at outlet of basin i.e. Purchuwarghat (Stn id 630) for the study period from (2000 to 2020) on Sunkoshi River basin

CHAPTER FIVE: RESULT AND DISCUSSION

5.1 Model Calibration and Validation

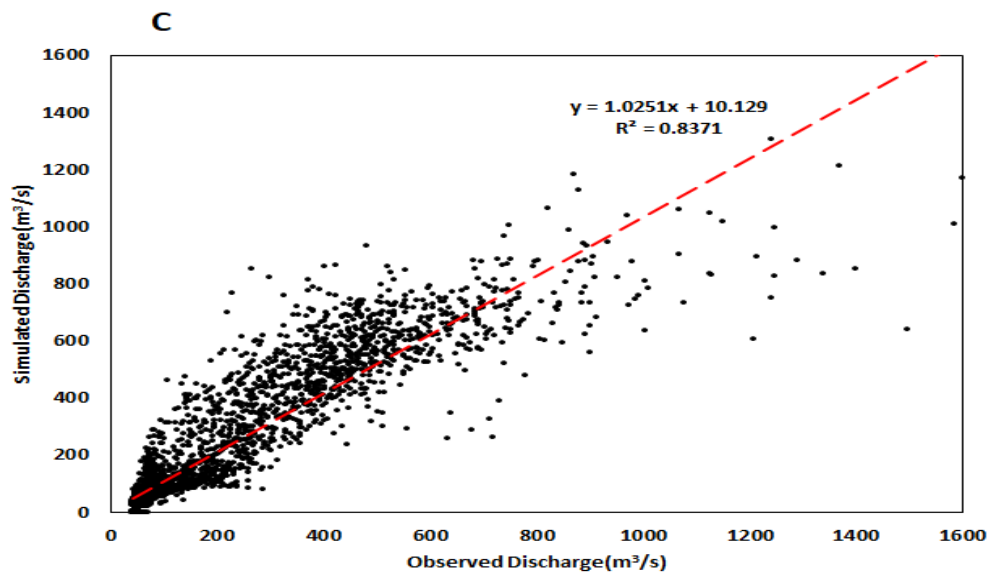
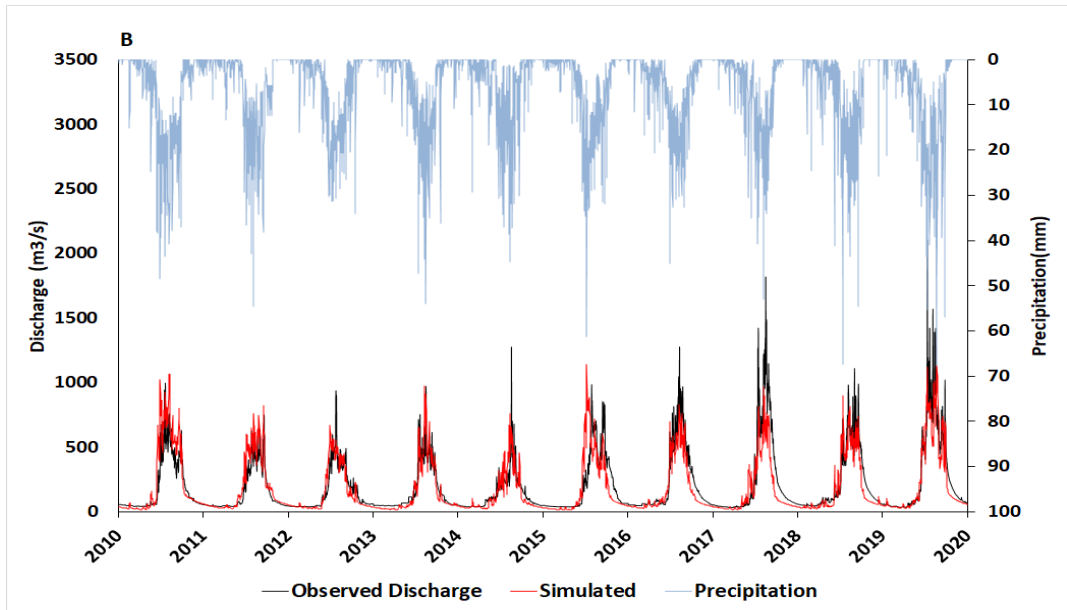
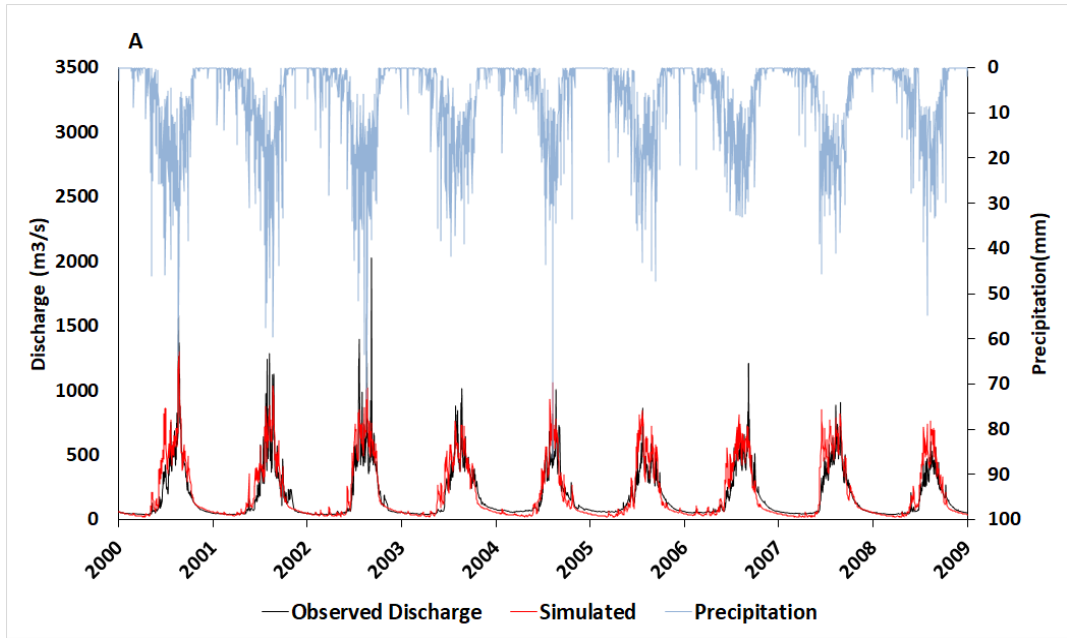
In the GDM, the main parameters that require adjustment are the positive degree-day factors, snow and rain coefficients, and recession coefficients. To optimize the model, various positive degree-day factors are applied, each specific to different months and falling within the estimated range of degree-day factors observed on various glaciers in the Nepal Himalayas. Similarly, the model undergoes calibration for snow and ice coefficients, as well as recession coefficients. All the calibrated parameters and coefficient used for the model calibration is listed in Table 5.1.

Daily simulated discharge is compared with the observed discharge hydrograph of Sunkoshi River basin at Purchuwarghat for the both calibration and validation period (Figure 5.1). Simulated discharge by the model is consistent with both the high and low observed discharge at the Purchuwarghat. A slight overestimation in the pre-monsoon or low-flow period by the model could be attributed to the way precipitation is distributed. The translation of precipitation data from lower elevation stations to higher altitudes might not reflect the true conditions; typically, high-altitude precipitation is over twice as much and can, in extreme instances, reach up to ten times higher levels (Immerzeel et al., 2015).

Table 5. 1: Calibrated parameters for GDM in Sunkoshi River basin

Parameters		SRB
Critical temperature		2 °C
Temperature lapse rate		0.006 °C/m
Recession coefficient		0.70
latitude : Geographical coordinate system at the centroid study area		28.05
Runoff coefficient	Land use type 1	0.3-0.6
	Land use type 2	0.5-0.7
	Land use type 3	0.5-0.6
	Land use type 4	0.3-0.6
	Land use type 5	0.95
	Land use type 6	0.95
	Land use type 7	1.00
	Land use type 8	1.00
Interception Threshold		1-8
Degree day factor	Snow melt	7–8.5 mm °C ⁻¹ day ⁻¹
	Ice melt	8–10.5 mm °C ⁻¹ day ⁻¹
	Ice under debris	3 mm °C ⁻¹ day ⁻¹
delay time of the overlying geologic formations (days).	$\delta_{gw,sh}$	20 days
Recession constant for shallow aquifer.	$\alpha_{gw,sh}$	0.50
delay time or drainage time of the deep aquifer geologic formations (days).	$\delta_{gw,dp}$	100 days
Recession constant for deep aquifer	$\alpha_{gw,dp}$	0.50
coefficient of shallow aquifer percolation to deep aquifer	β_{dp}	0.80

Precipitation gradients in mountainous environments, vary both vertically and horizontally (Barry, 2012). The complex terrain of the Himalayan region, at altitudes can have an influence, on how and when precipitation's distributed in terms of space and time, posing challenges in representing precipitation patterns(Kayastha & Kayastha, 2019). Nevertheless, despite these limitations, the model successfully simulates daily discharge, achieving favorable NSE and R² values and maintaining a volume difference below ±10%, even with limited input data.



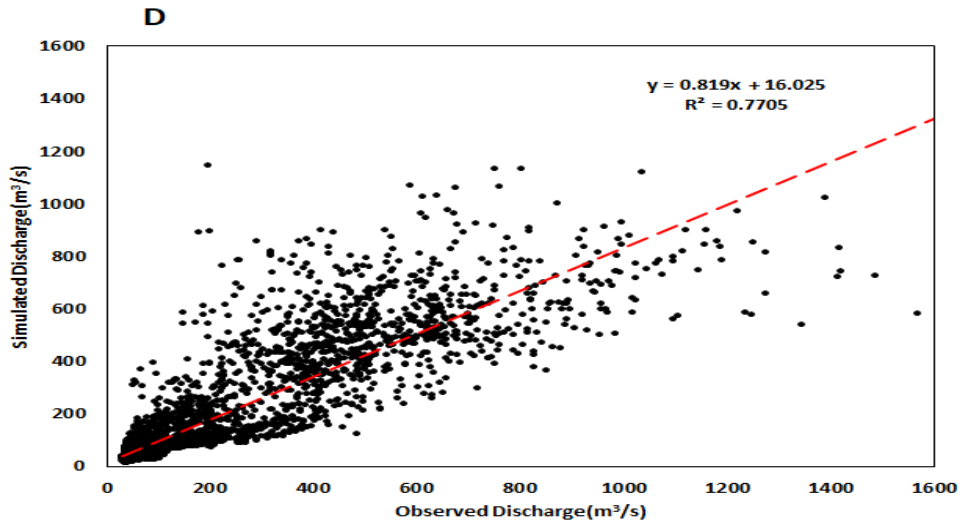


Figure 5. 1: (A) Precipitation distribution and observed vs Simulated discharge for calibration period (2000-2009) ,(B) Precipitation distribution and observed vs Simulated discharge for validation period (2010-2020), (C) Scatter plots between the observed and simulated values for the calibration period (2000-2009), (D) Scatter plots between the observed and simulated values for the validation periods.(2010-2020).

The model's performance is evaluated using the optimal parameters for the basin. In Sunkoshi river basins, the Nash-Sutcliffe Efficiency (NSE) values are 0.79 and 0.77 for calibration and validation periods, and the volume difference remains within $\pm 10\%$. Moreover, the coefficient of determination (R^2) reaches values of 0.83 and 0.77 in both cases. The model's performance is deemed satisfactory as indicated in the Table 5.2. Figure 5.1.C, D shows an (R^2) of 0.8371 and 0.7705 between simulated discharge and observed discharge indicates that approximately 83.71% and 77.05% of the variability in the observed discharge in calibration and validation can be explained by the variability in the simulated discharge using this model. It also indicates a better fit of the model to the observed data.

Table 5. 2:NSE ,volume difference and R^2 of GDM in Sunkoshi River basin

Performance Index	SRB	
	Calibration	Validation
NSE	0.79	0.77
Vol.diff %	-8	-9.8
R^2	0.83	0.77

5.2 Contribution of Snowmelt, Icemelt, Rain and Baseflow

Subsequently, a detailed examination is conducted on the model's outcomes, specifically focusing on the various constituents of discharge. Figure 5.2 illustrates the average monthly contributions of snowmelt, ice melt (both clean and debris-covered), rainfall, and baseflow on discharge during the calibration and validation periods for SRB. In SRB, snowmelt accounts for 9.68% of the total annual discharge, clean ice and ice melt beneath debris contribute 2.5%, rainfall constitutes 50.15%, and baseflow makes up 37.66% during the calibration period. In SRB, snowmelt accounts for 11.38% of the total annual discharge, clean ice and ice melt beneath debris contribute 3%, rainfall constitutes 48.26%, and baseflow makes up 37.33% during the validation period. Upon analyzing the average monthly contribution, we discover during low flow period in both calibration and validation between May to June there is significant contribution of icemelt and snowmelt on the stream runoff highlighting the importance of snowmelt and icemelt on river discharge during low flow period. With increase in temperature there will be less snow fall and the decrease in glacier coverage resulting the negative impact on discharge during low flow period. Rainfall exerts a dominant influence on discharge during the monsoon period (June–September) in river basins, while baseflow maintains a consistent contribution throughout the year, peaking in the late monsoon period. The contribution of ice melt to discharge commences in the pre-monsoon period, with peak contributions occurring from May to October in basins, influenced by temperature and precipitation patterns. By Khanal et al. (2021) and Wijngaard et al. (2017) in Narayani River basin using SPHY model the contribution of rain runoff was 63%-65%, snowmelt 9%-12% , icemelt was 3%-4% , and base flow was 21%. This research intently matches contribution from snowmelt and icemelt, besides the contribution of rain and baseflow is varied this may be due to the area coverage of the basin i.e. the Narayani basin is about 37 times bigger than our study area river basin. Our result aligns with their result in similar manner. Similarly, when comparing the contribution of ice melt in our study to the research conducted by Kayastha & Kayastha (2019) on the Trishuli River basin, which indicated a 12% ice melt contribution to the total discharge within an area of 623 km², our findings align closely, showing approximately 9%. This similarity is despite our study area having a glaciated area almost three times smaller than that of the Trishuli River basin.

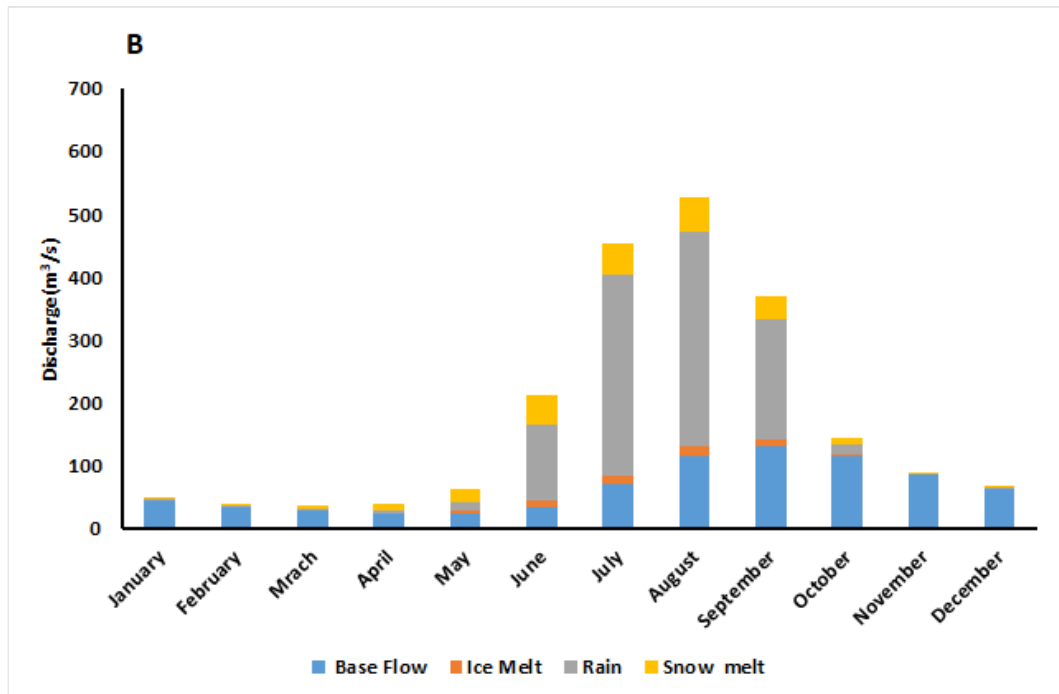
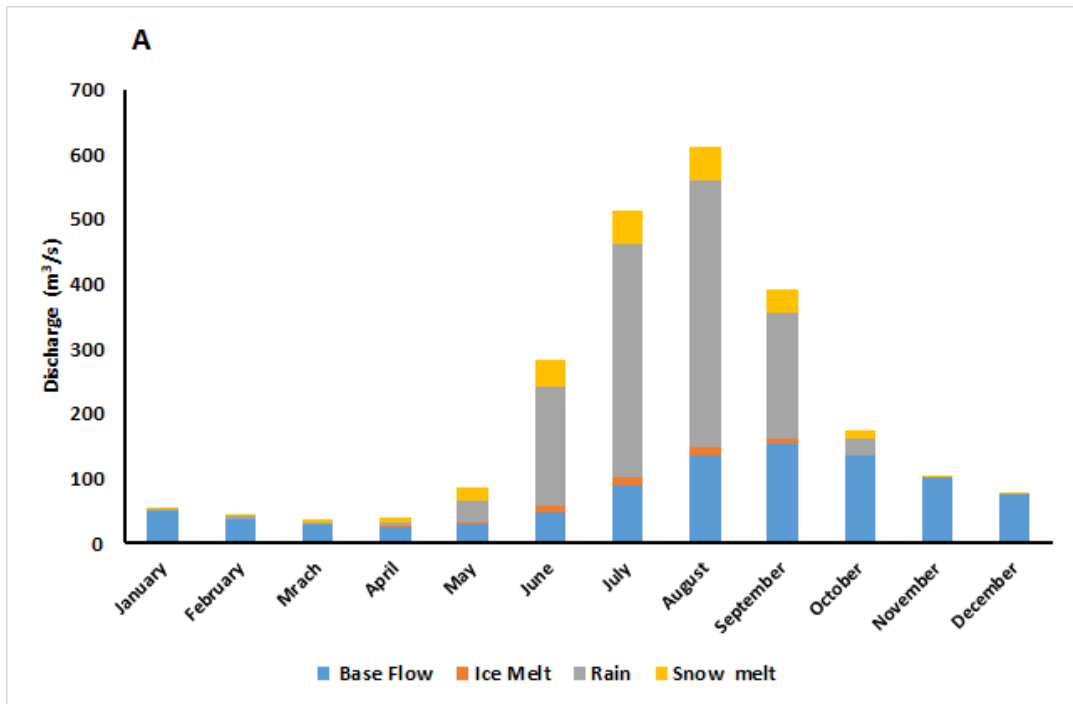


Figure 5. 2: (A) Average monthly discharge contribution graph of baseflow,rain,snowmelt, and icemelt of calibration period (2000-2009). (B) Average monthly discharge contribution graph of baseflow, rain, snowmelt, and icemelt of validation period (2010-2020).

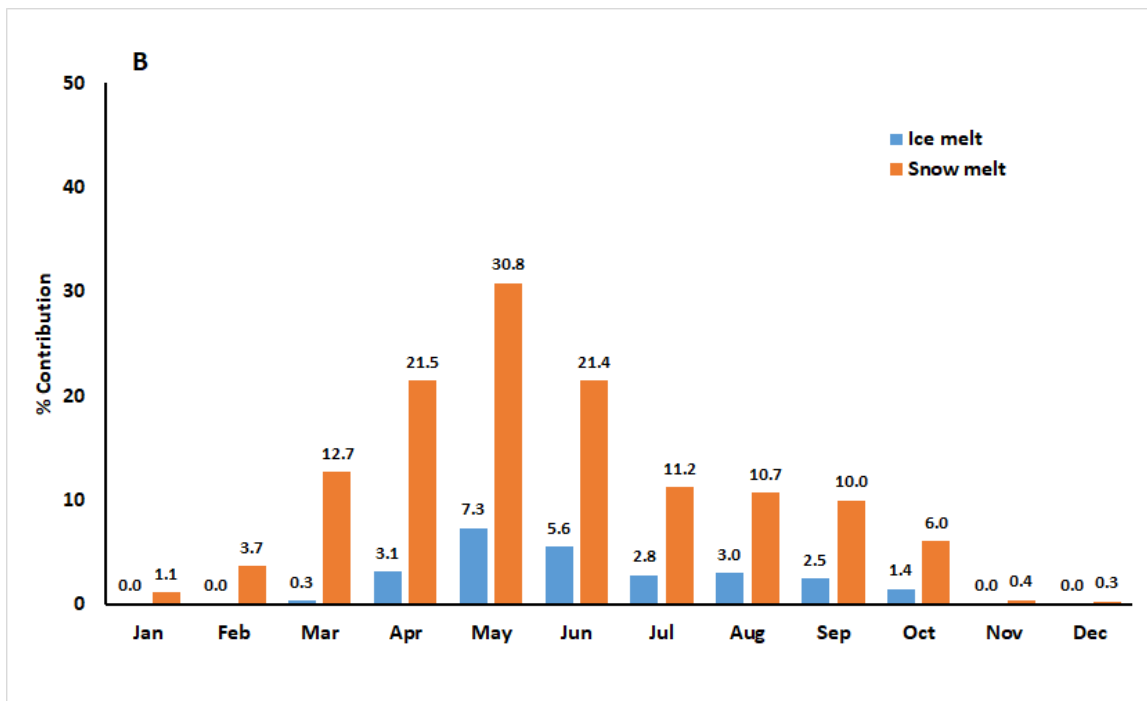
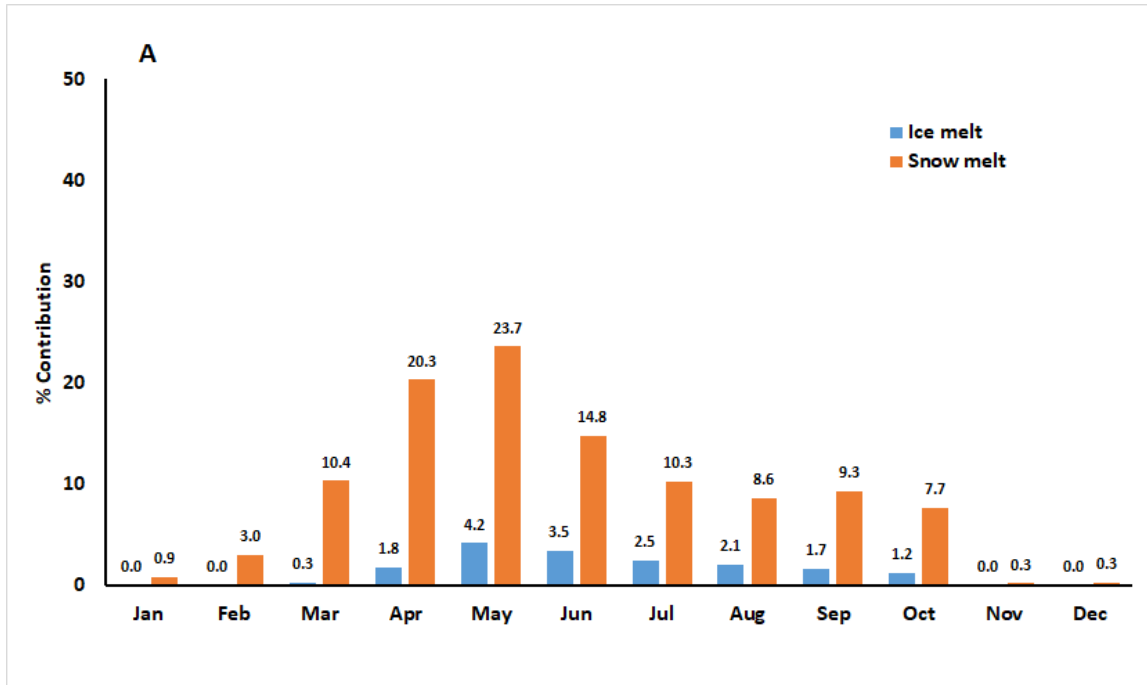


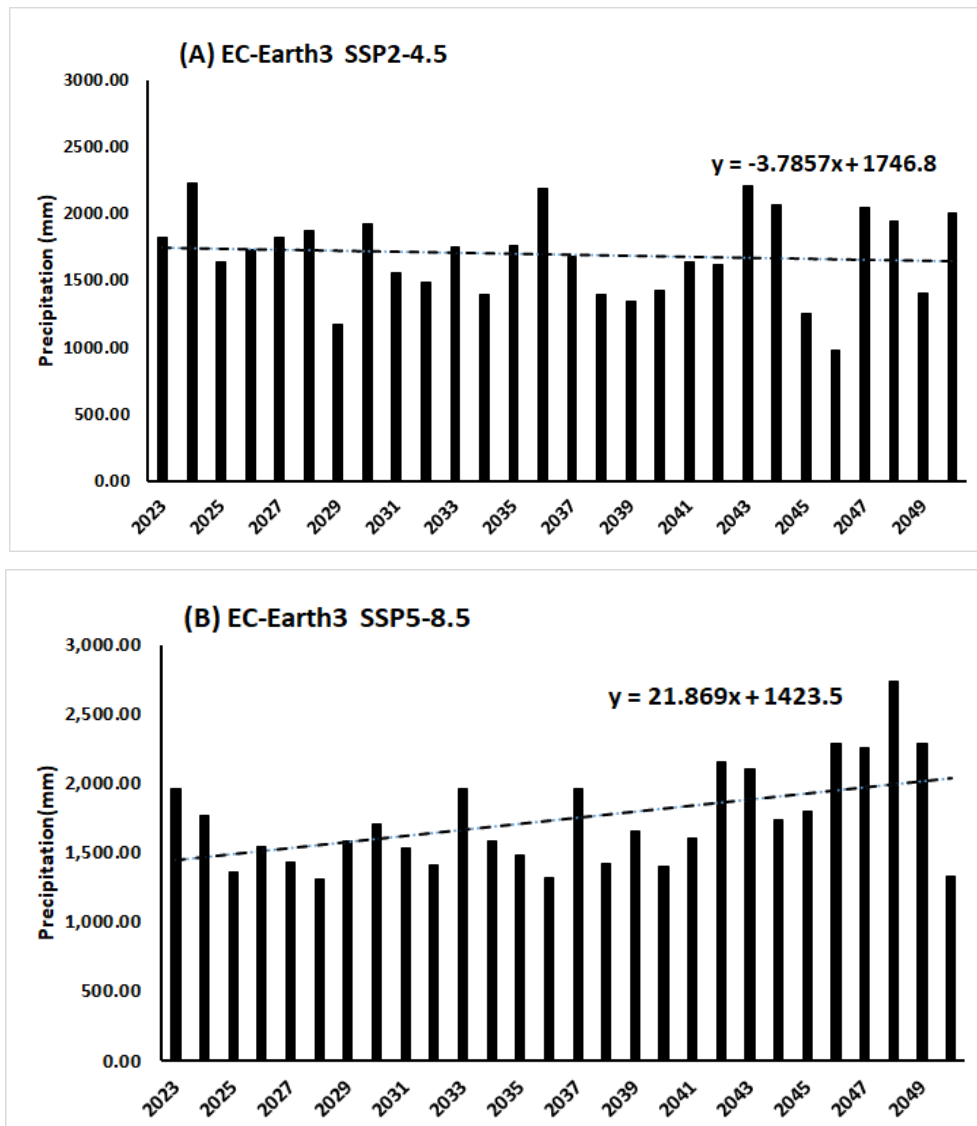
Figure 5. 3 (A)Average monthly percentage contribution graph of Snowmelt and Icemelt for calibration period (2000-2009) (B)Average monthly percentage contribution graph of Snowmelt and Icemelt for validation period (2010-2020)

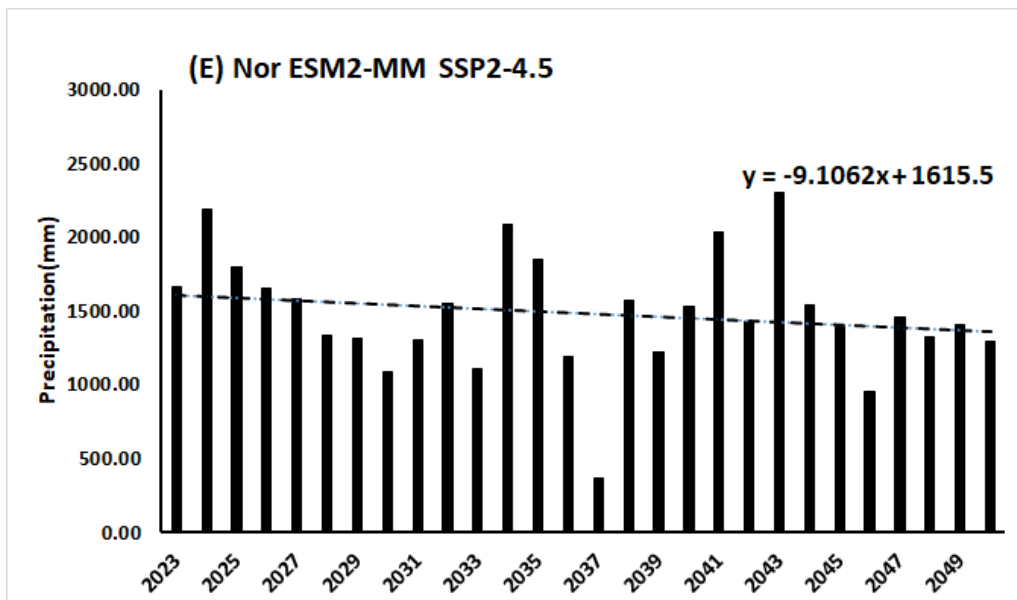
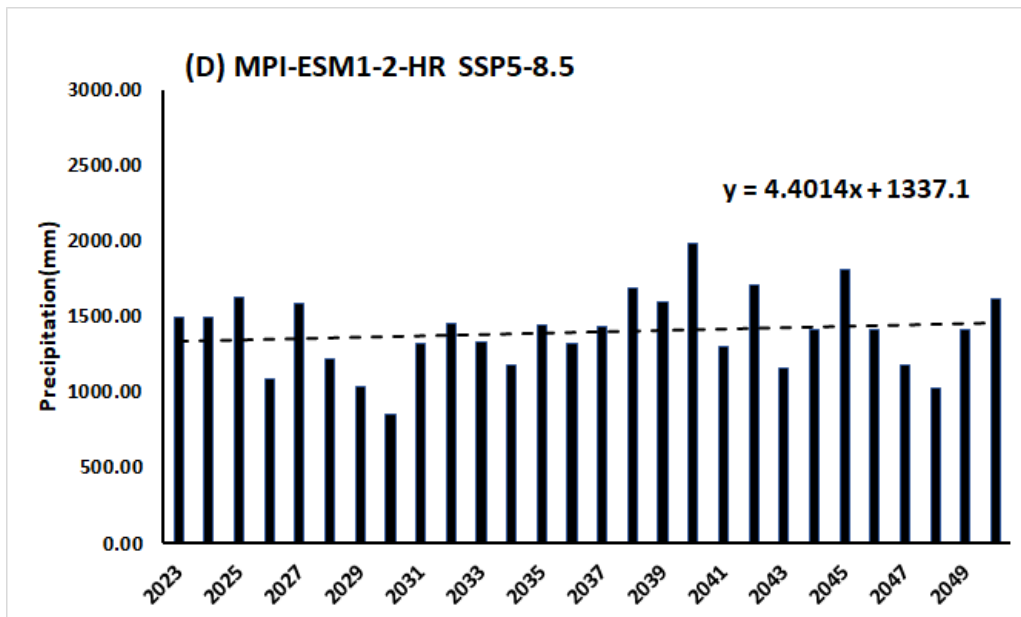
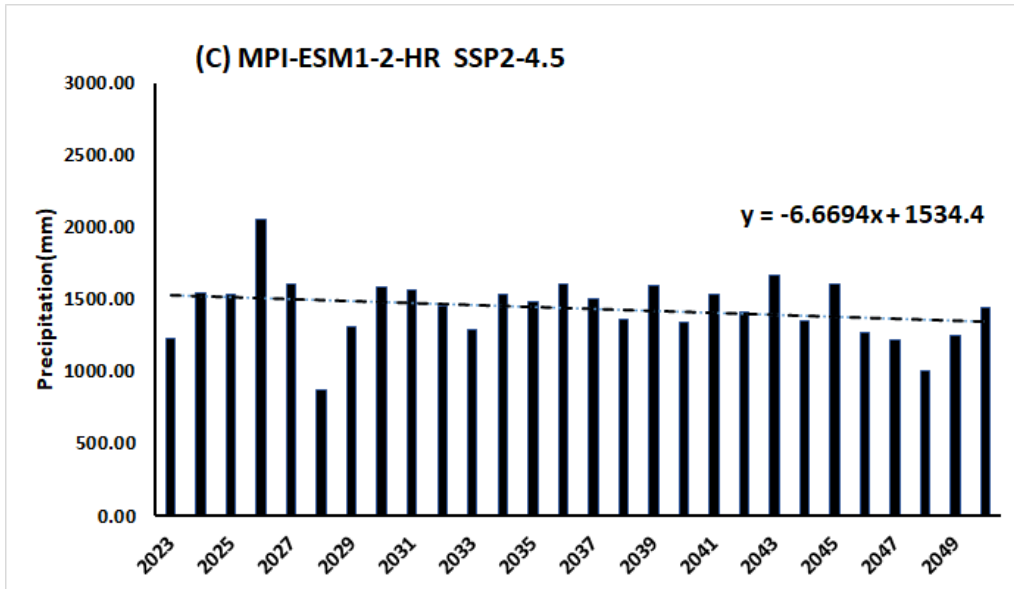
Figure 5.3 shows monthly variation in percentage contribution of icemelt and snowmelt. During low flow period in between May to June there is significant contribution of icemelt and snowmelt on the stream runoff. Icemelt and snow melt contribution at validation period shows the increasing pattern from calibration period. during low flow period

highlighting the importance of snowmelt and icemelt on river discharge on that period. Rising temperatures could lead to reduced snowfall and glacier coverage to the point it, negatively impacting river discharge in future.

5.3 Future Prediction

The future climate analysis covering the years from 2023 to 2050, a 27-year period has been carried out. Our projections don't reach beyond 2050 due to the absence of considerations for future land cover changes in our study. Our model is fundamentally descriptive, allowing us to simulate the future trends of various glacial melts and other physical components within the basin. To forecast future discharge, we've integrated the average daily temperature and daily precipitation data from the three Global Circulation Model (GCM) into the GDM. (Figure 5.3,5.4)





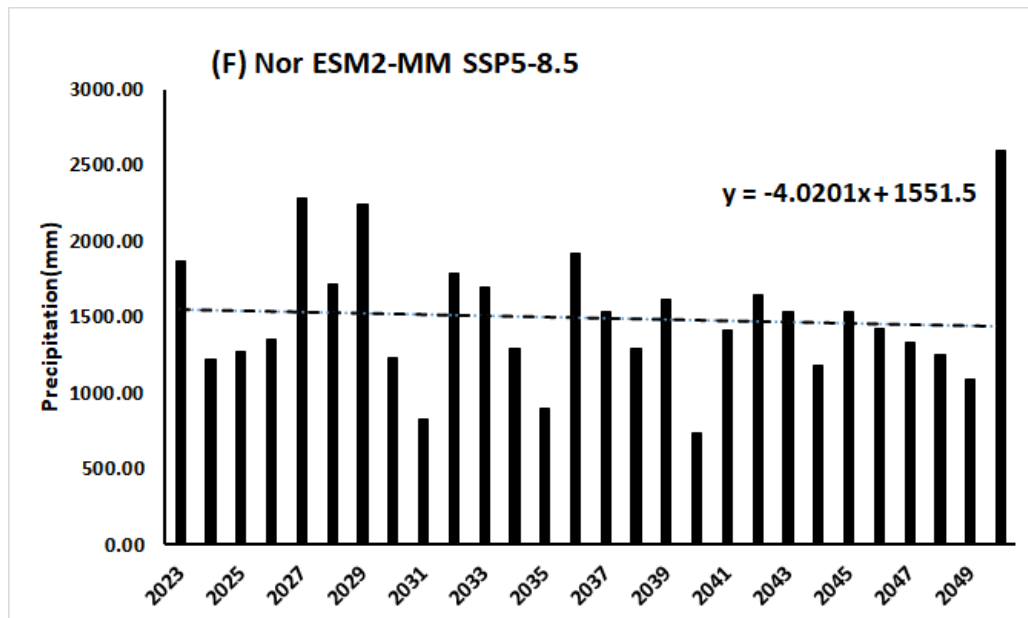
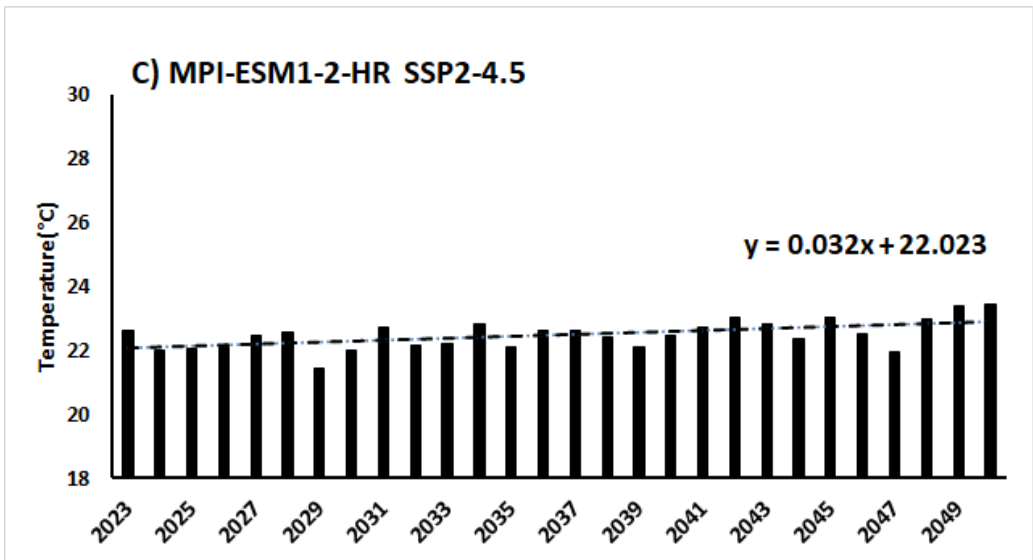
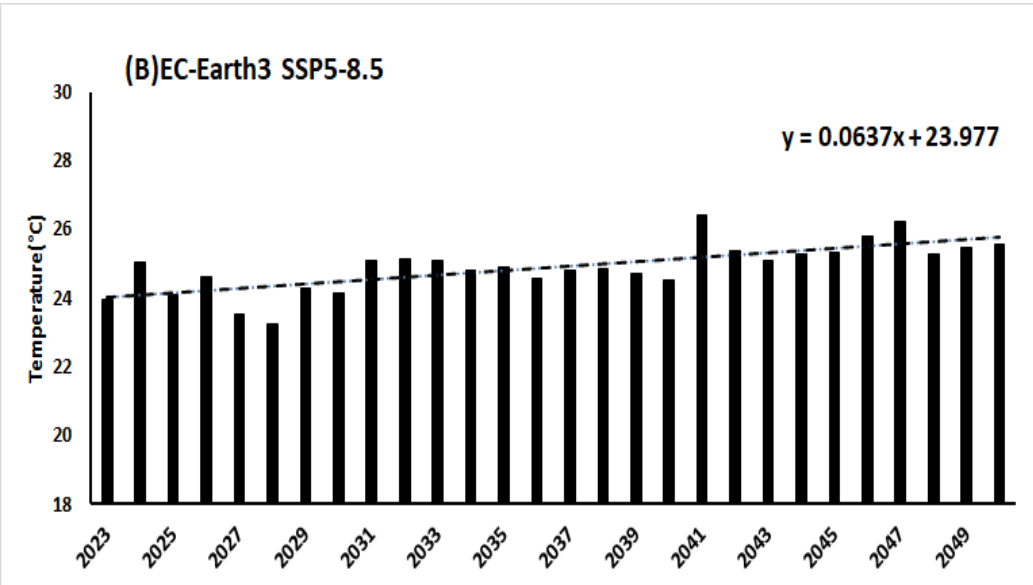
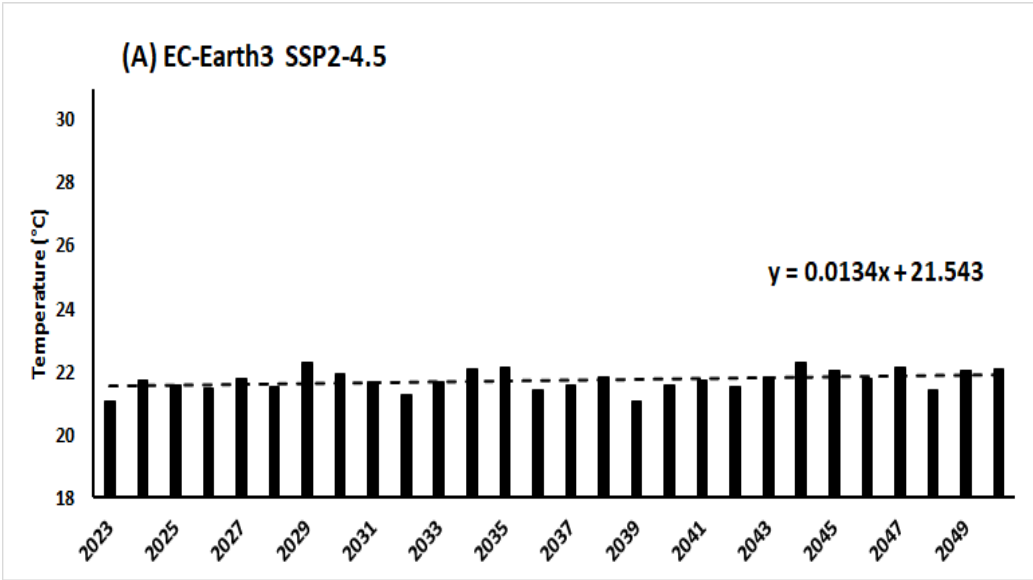


Figure 5. 4: (A) Future total annual precipitation variation under EC-Earth3 GCM SSP24.5 scenario (2023-2050) (B) Future total annual precipitation variation under EC-Earth3 GCM SSP58.5 scenario (2023-2050) (C) Future total annual precipitation variation under MPI-ESM1-2-HR GCM SSP24.5 scenario (2023-2050) (D) Future total annual precipitation variation under MPI-ESM1-2-HR SSP58.5 scenario (2023-2050) (E) Future total annual precipitation variation under Nor ESM2-MM GCM SSP24.5 scenario (2023-2050) (F) Future total annual precipitation variation under Nor ESM2-MM SSP58.5 scenario (2023-2050).

Interestingly, precipitation exhibits declining trends in SRB under SSP24.5 scenarios, projected at rates of 3.78 mm/year, 6.67 mm/year, and 9.11 mm/year by GCMs EC-Earth3, MPI-ESM1-2HR, and Nor-ESM2-MM, respectively. Conversely, under SSP58.5 scenarios, EC-Earth3 forecasts a notable increase in precipitation at a rate of 21.87 mm/year, while MPI-ESM1-2HR indicates a slight increase at 4.40 mm/year. However, within the SSP58.5 scenarios, Nor-ESM2-MM projects a decrease in precipitation at a rate of 4.02 mm/year. This anticipated decline in precipitation rates could consequently lead to a reduction in simulated future discharge.



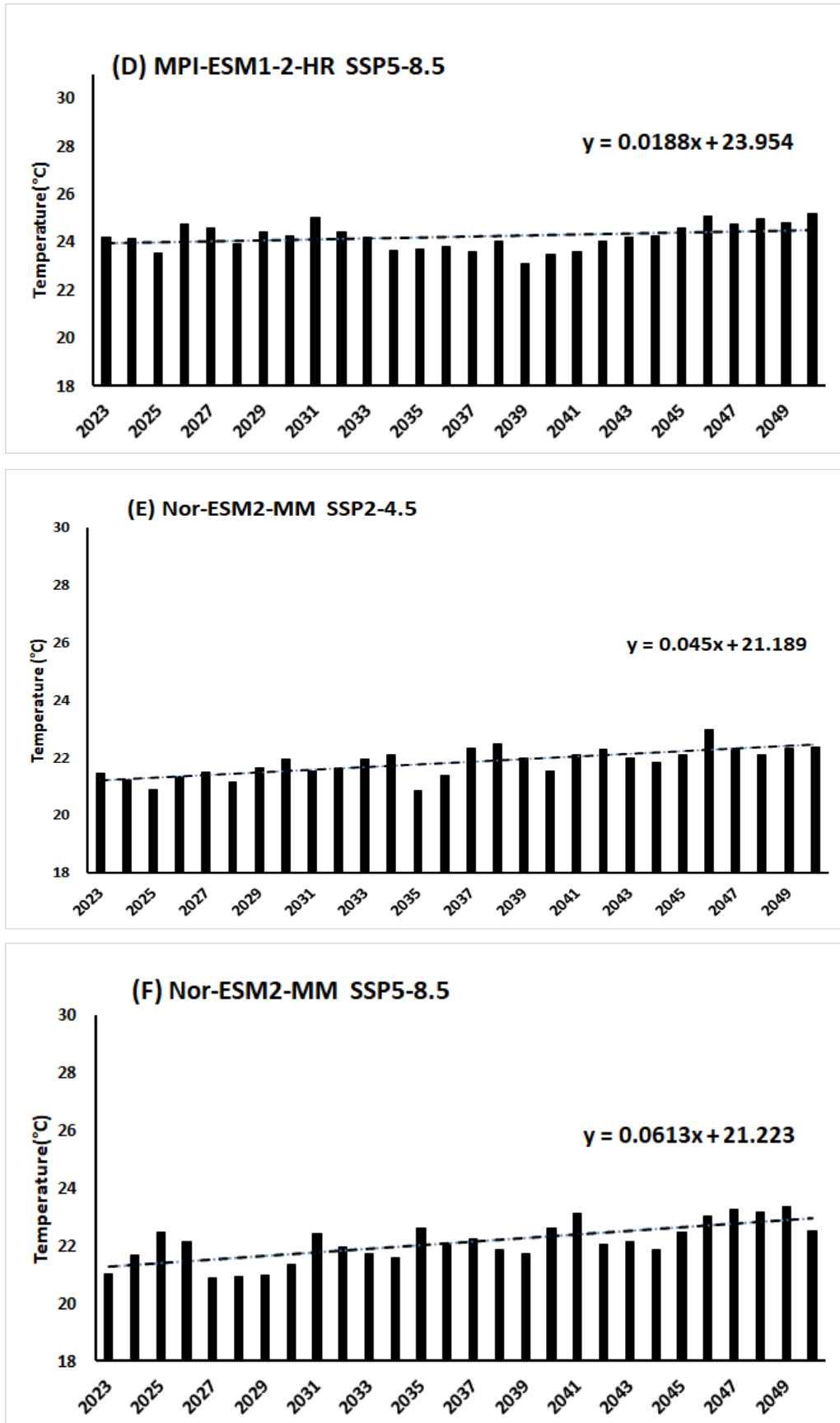


Figure 5. 5:(A) Future average annual temperature variation at base station under EC-Earth3 GCM SSP24.5 scenario (2023-2050) (B) Future average annual temperature

variation at base station under EC-Earth3 GCM SSP58.5 scenario (2023-2050) (C) Future average annual temperature variation at base station under MPI-ESM1-2-HR GCM SSP24.5 scenario (2023-2050) (D) Future average annual temperature variation at base station under MPI-ESM1-2-HR SSP58.5 scenario (2023-2050) (E) Future average annual temperature variation at base station under Nor ESM2-MM GCM SSP24.5 scenario (2023-2050) (F) Future average annual temperature variation at base station under Nor ESM2-MM SSP58.5 scenario (2023-2050)

Figure 5.5 shows the temperature shifts vary among scenarios and models. In the SSP 24.5 scenario, GCM EC-Earth3 shows no significant trend, whereas MPI-ESM1-2HR and Nor-ESM2-MM display increasing trends at rates of 0.03°C/year and 0.045°C/year, respectively. Similarly, in the SSP58.5 scenarios, EC-Earth3 predicts a rising temperature trend at a rate of 0.063°C/year, followed by Nor-ESM2-MM at 0.061°C/year. However, under SSP58.5, MPI-ESM1-2HR maintains a consistent temperature change at a rate of 0.019°C/year (Table 5.3). This anticipated increase in temperature rates might reduce snowmelt contributions while amplifying the impact of ice melt in the future.

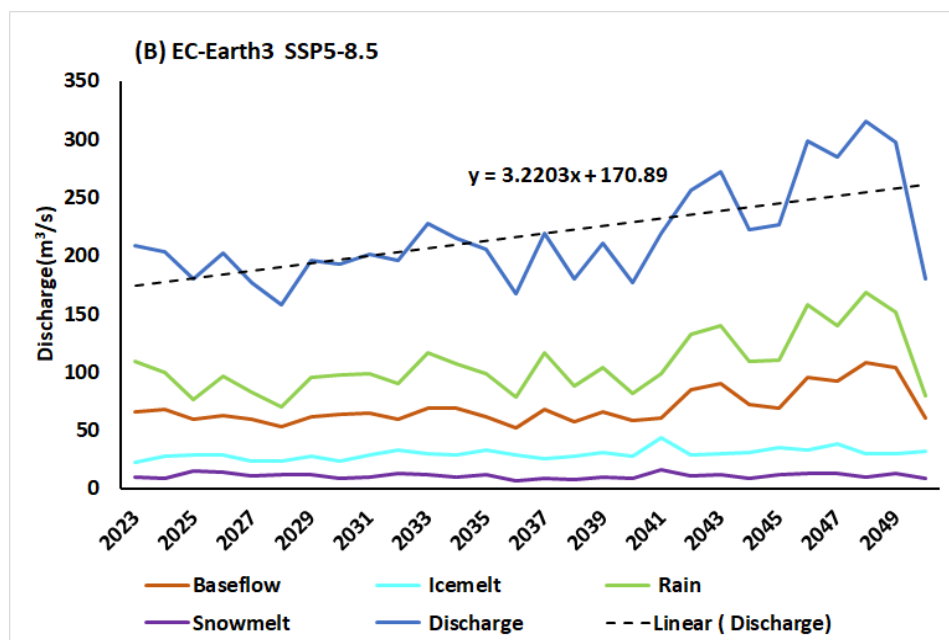
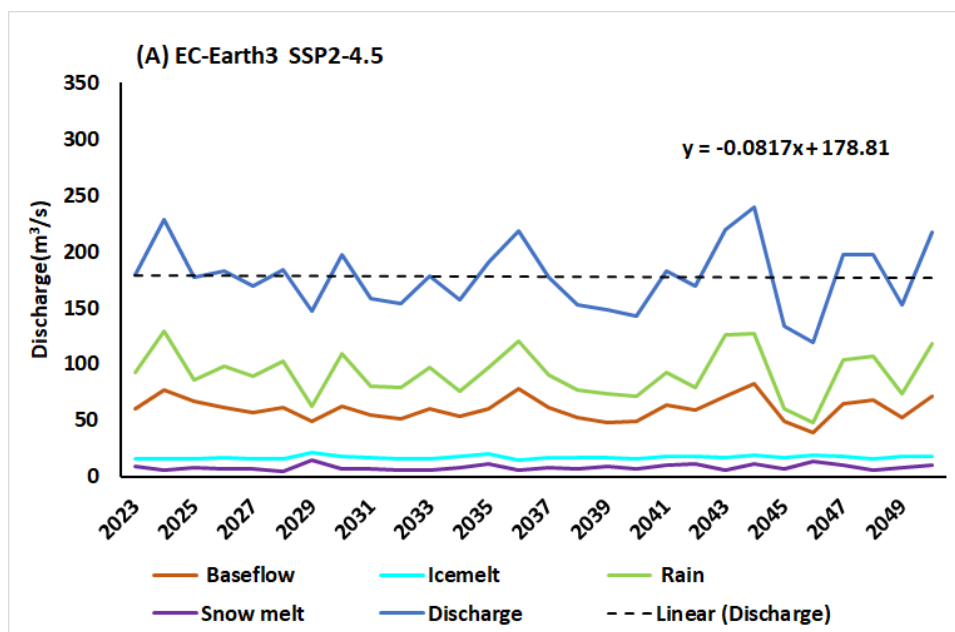
Table 5. 3 Precipitation and Temperature trend per year up to 2050

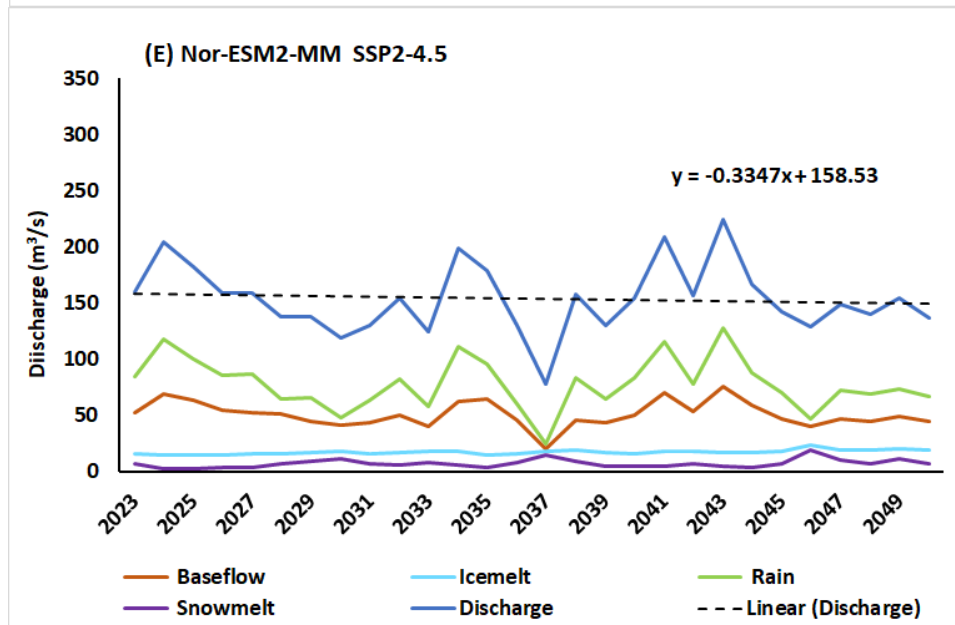
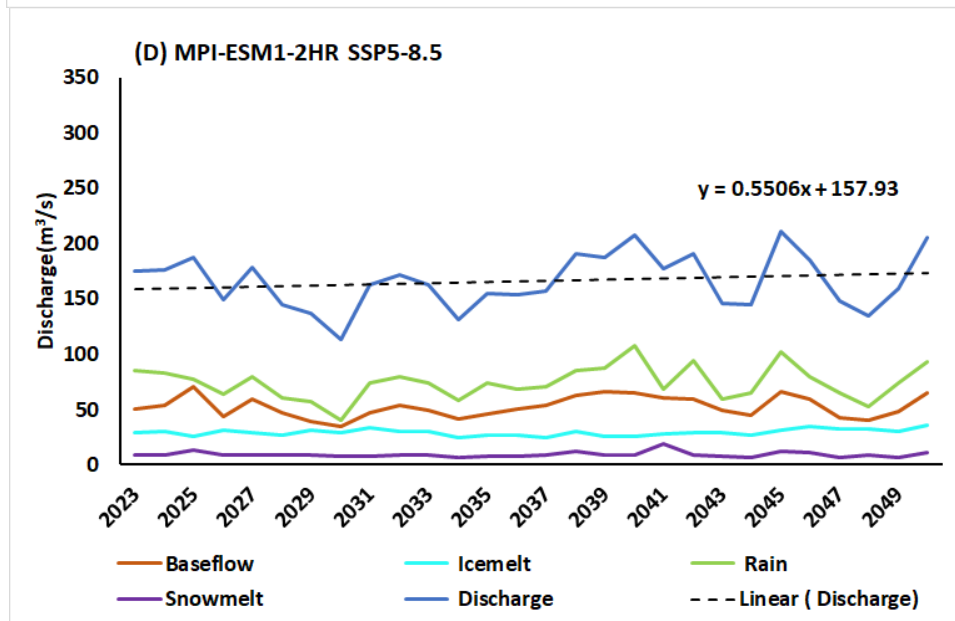
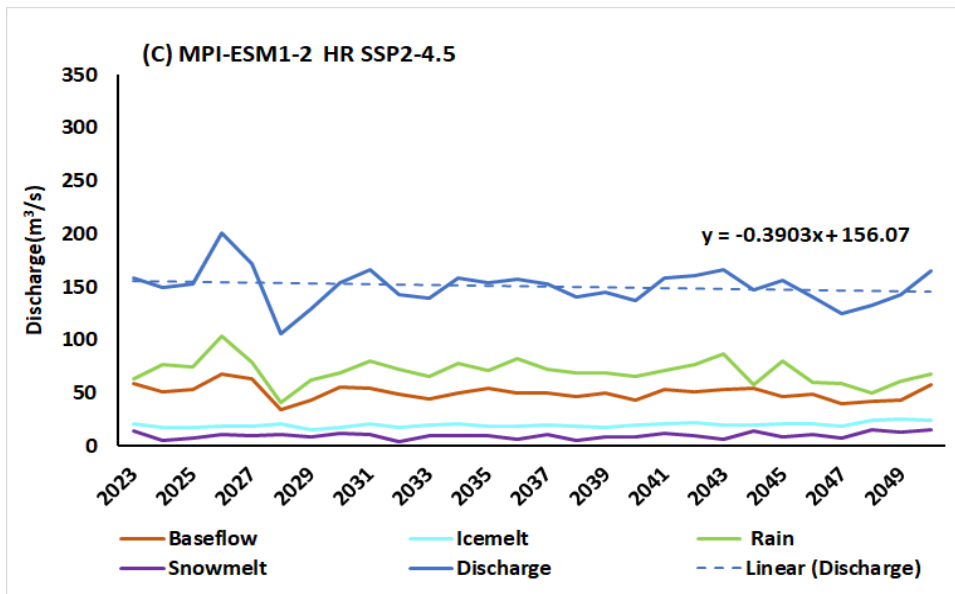
S. No	GCM	Change in Trend	Scenario	
			SSP24.5	SSP58.5
1	EC-Earth3	Precipitation Trend (mm/yr)	-3.78	21.87
		Temperature(°C/yr)	0.01	0.06
2	MPI-ESM1-2HR	Precipitation Trend (mm/yr)	-6.67	4.40
		Temperature(°C/yr)	0.03	0.018
3	Nor ESM2-MM	Precipitation Trend (mm/yr)	-9.1	-4.02
		Temperature(°C/yr)	0.045	0.061

5.3.1 Contribution of streamflow components to the future discharge

In Figure 5.6, within the context of the SSP24.5 scenario projected by GCM EC-Earth3, there is a noticeable 0.0817 m³/s decrease in total discharge. Interestingly, the contribution of baseflow to the total discharge doesn't exhibit a significant upward trend. Analyzing the

contributions of different constituents, baseflow averages at 34.04%, ice-melt at 10%, rain at 51.13%, and snowmelt at 4.84%. This lack of increase may be linked to declining precipitation and rising temperatures. Rainfall remains the primary contributor to total discharge. Conversely, under the SSP58.5 scenarios by GCM EC-Earth3, there's a clear 3.22 m³/s increase in total discharge (Table 5.4). Notably, the baseflow contribution to total discharge displays a distinct upward trend. Examining various constituents, baseflow averages at 32.07%, icemelt at 14%, rain at 48.8%, and snowmelt at 5.13% (Table 5.5). Once more, snowmelt appears less impactful, likely due to increasing daily average temperatures, while rainfall exhibits a significant upward trend.





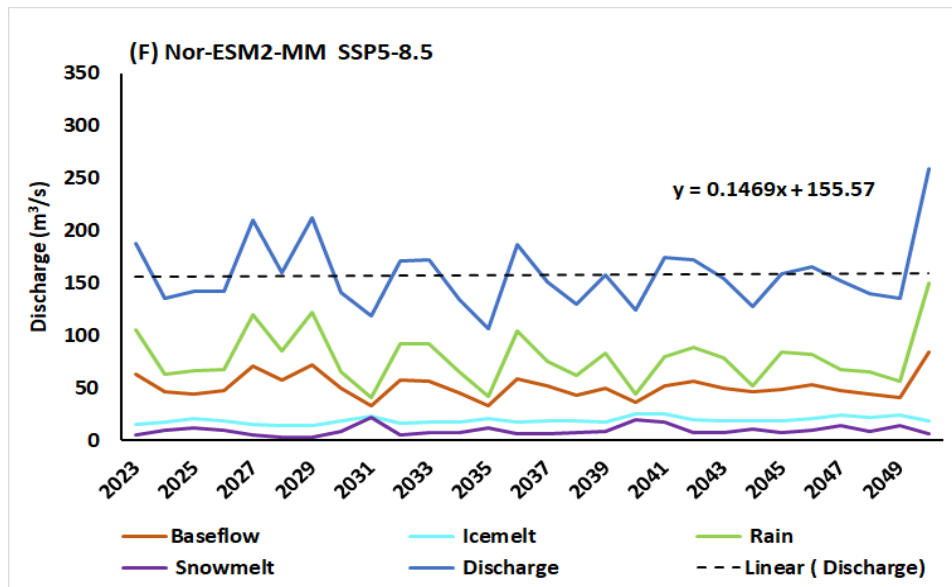


Figure 5. 6:(A) Average annual contribution in future discharge under EC-Earth3 GCM SSP24.5 scenario (2023-2050) (B) Average annual contribution in future discharge under EC-Earth3 GCM SSP58.5 scenario (2023-2050) (C) Average annual contribution in future discharge under MPI-ESM1-2-HR GCM SSP24.5 scenario (2023-2050) (D) Average annual contribution in future discharge under MPI-ESM1-2-HR SSP58.5 scenario (2023-2050) (E) Average annual contribution in future discharge under Nor ESM2-MM GCM SSP24.5 scenario (2023-2050) (F) Average annual contribution in future discharge under Nor ESM2-MM SSP58.5 scenario (2023-2050)

For MPI-ESM1-2HR in SSP24.5 scenarios, there's a slight decline in the total simulated discharge trend, decreasing at a rate of $0.3903 \text{ m}^3/\text{s}$. This decrease coincides with a diminishing trend in rainfall contribution, while baseflow remains relatively stable. There's also a slight uptick in the trend of snowmelt. Looking at constituent contributions, baseflow averages at 33.45%, ice-melt at 13.37%, rain at 46.51%, and snowmelt at 6.66%. In SSP58.5 scenarios, there are no significant trends observed in baseflow, rain, snowmelt, or ice melt. However, the total discharge demonstrates an increasing trend, reaching $0.55 \text{ m}^3/\text{s/day}$ for MPI-ESM1-2HR. Constituent contributions remain relatively consistent, with baseflow at 31.62%, ice-melt at 18.12%, rain at 44.56%, and snowmelt at 5.71%.

Under the SSP24.5 scenarios, Nor-ESM2-MM indicates a slight $0.3347 \text{ m}^3/\text{s}$ decrease in the total simulated discharge trend. This decrease aligns with a declining trend in rainfall contribution, stable baseflow, and a slight uptick in snowmelt. Looking at constituent contributions, baseflow averages at 32.99%, ice-melt at 11.85%, rain at 49.90%, and

snowmelt at 5.62%. In SSP58.5 scenarios, baseflow, rain, snowmelt, and ice melt show no significant trends. Nevertheless, the total discharge exhibits an increasing trend, with Nor-ESM2-MM reaching 0.1469 m³/s. Analyzing constituent contributions, baseflow covers the average range of 32.34%, ice-melt 12.65%, rain 48.63%, and snowmelt 6.38%. This projected decrease in precipitation rates could lead to a reduction in simulated future discharge. The change discharge and percentage contribution project by three GCMs under SSP24.5 and SSP58.5 are depicted in Table 5.4 and 5.5

Table 5. 4. Future Discharge trend by 2050 (SSP24.5 and SSP58.5 scenarios)

Scenario	GCM	Discharge Trend (m ³ /s)
SSP24.5	EC-Earth3	-0.08
SSP58.5	EC-Earth3	3.22
SSP24.5	MPI-ESM1-2-HR	-0.39
SSP58.5	MPI-ESM1-2-HR	0.55
SSP24.5	Nor ESM2-MM	-0.33
SSP58.5	Nor ESM2-MM	0.14

Table 5. 5. Future Hydrological Component Contributions by 2050 (SSP24.5 and SSP58.5 scenarios)

Scenario	GCM	Rainfall (%)	Baseflow (%)	Icemelt (%)	Snowmelt (%)
SSP24.5	EC-Earth3	51.13	34.04	10	4.84
SSP58.5	EC-Earth3	48.80	32.07	14	5.13
SSP24.5	MPI-ESM1-2-HR	46.51	33.45	13.37	6.67
SSP58.5	MPI-ESM1-2-HR	44.56	31.62	18.12	5.71
SSP24.5	Nor ESM2-MM	49.90	32.99	11.85	5.62
SSP58.5	Nor ESM2-MM	48.63	32.34	12.65	6.38

In Figure 5.7 when assessing the average monthly contribution percentage to total discharge, the contribution of icemelt notably increases from validation period of about 7% to 46.5% and 54.1% under the SSP24.5 and SSP58.5 scenarios by 2050. Notably, ice melt consistently outpaces snowmelt in contributing to the overall discharge, showing an upward trend in ice melting year by year and day by day and the fact that due to the increment of the temperature in future there may be less snow fall and also increase in melting of ice causing the decrease in glacier coverage, which is a big threat for Himalayas and Himalaya's water system in upcoming days.

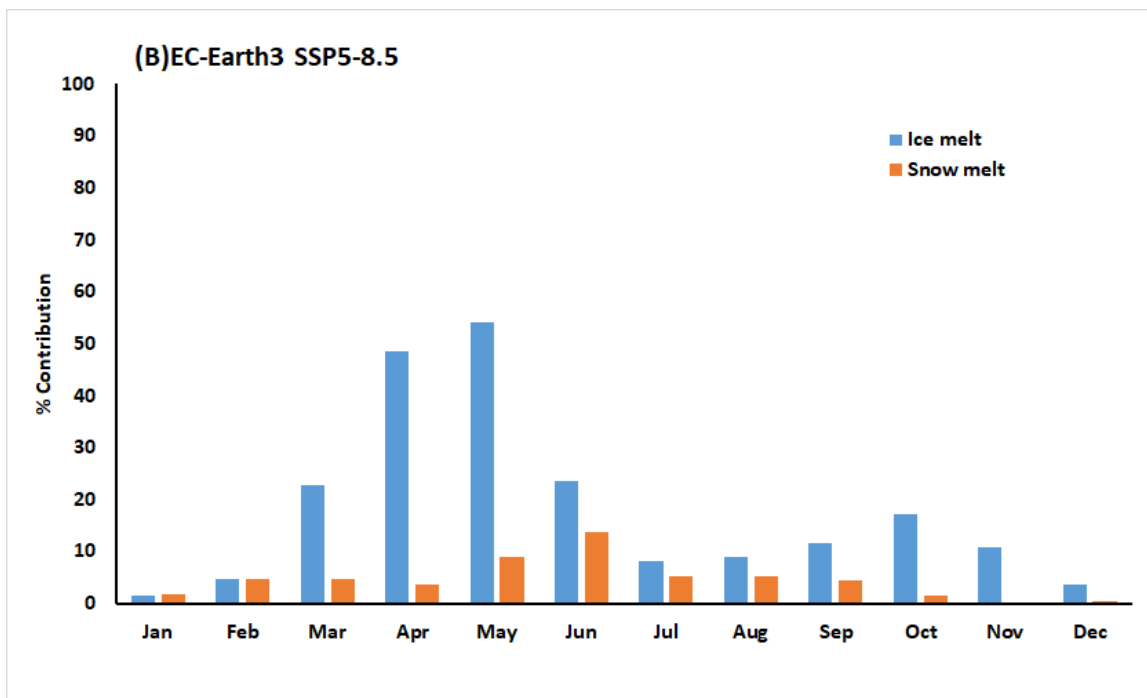
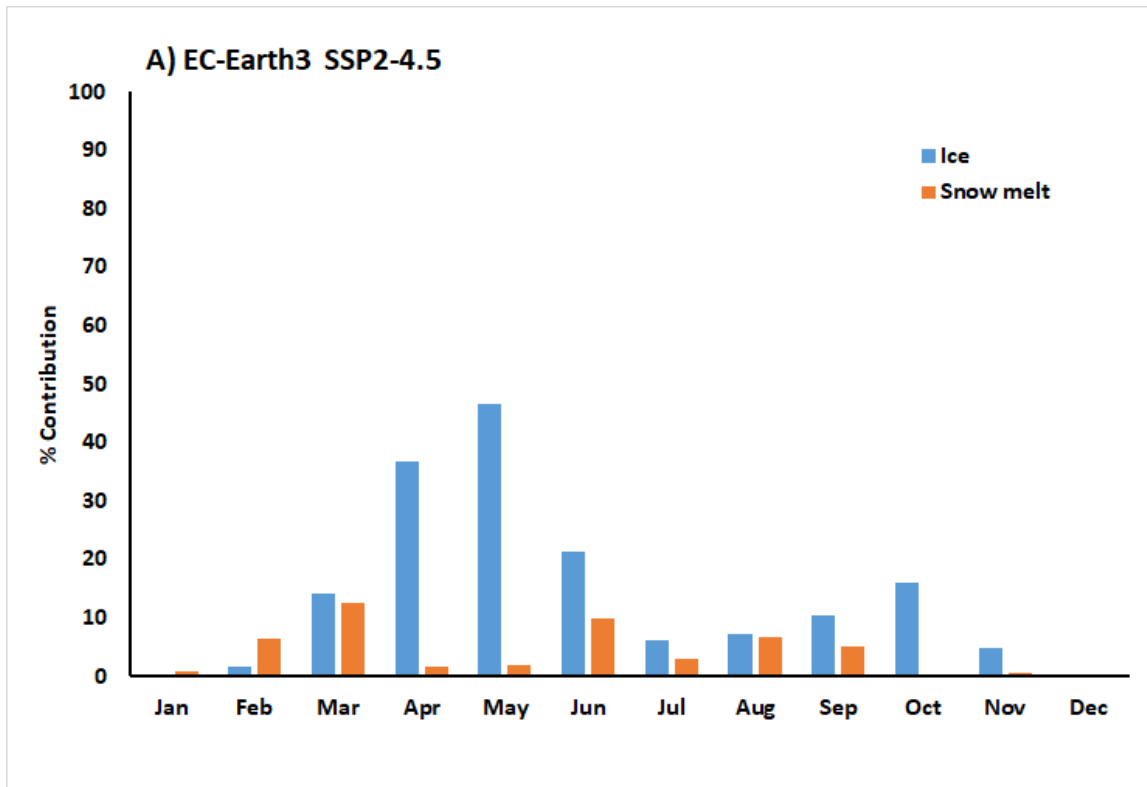


Figure 5. 7 (A)Average Monthly Contribution graph of Snowmelt and Icemelt under SSP24.5 (2023-2050) (B) Average Monthly Contribution graph of Snowmelt and Icemelt under SSP58.5 (2023-2050).

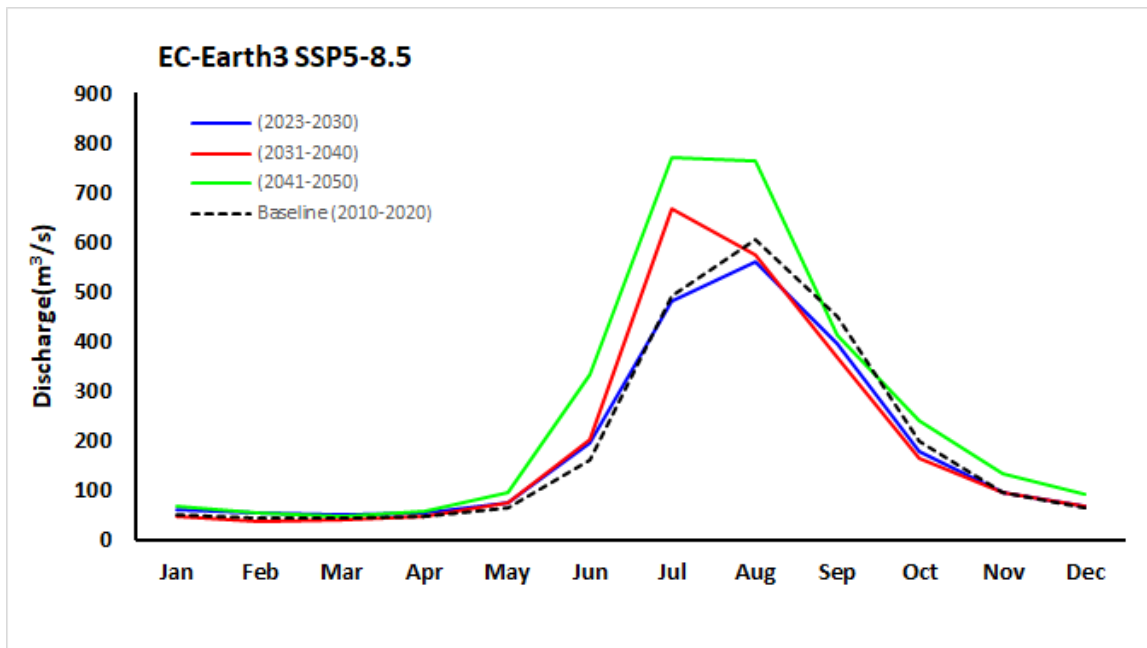
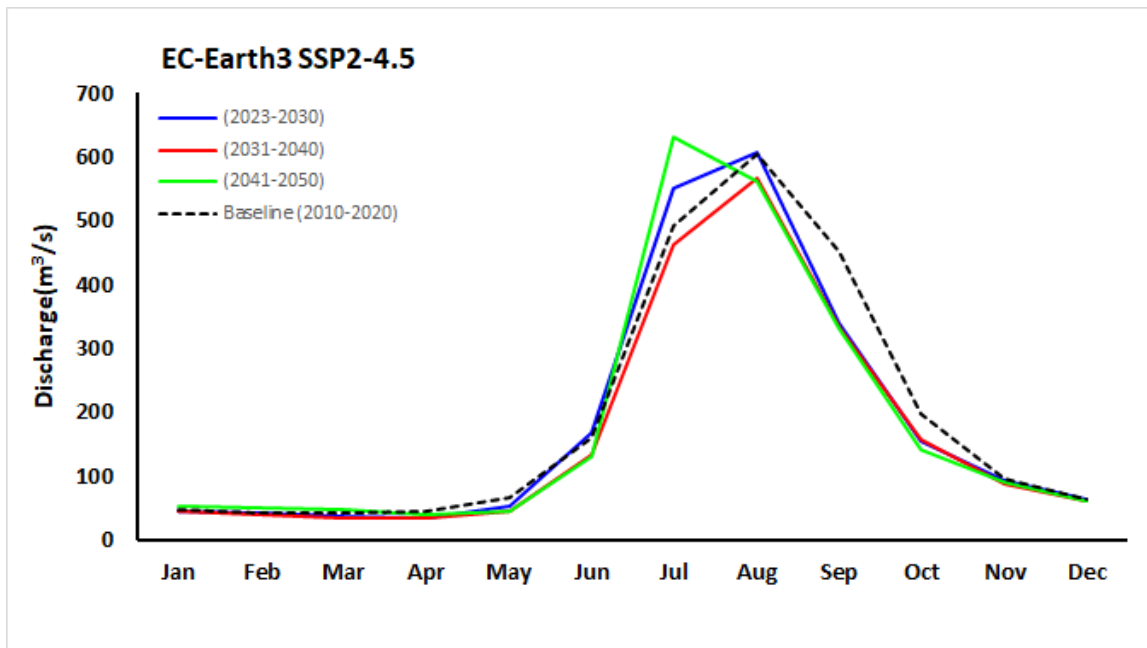
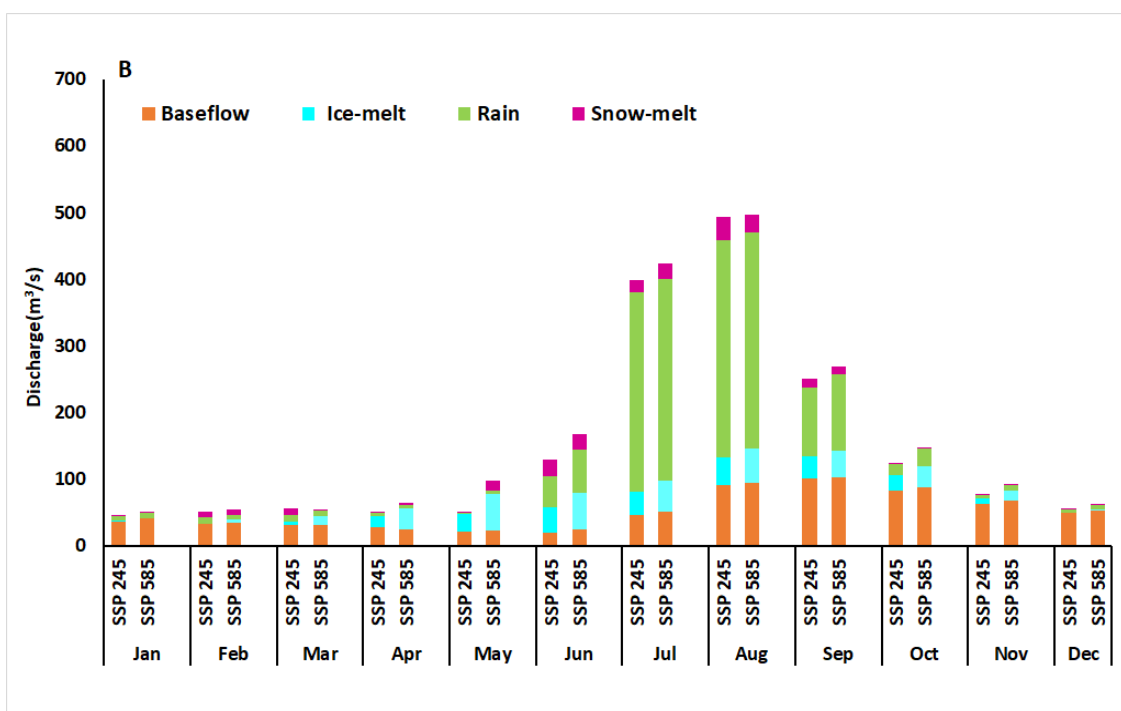
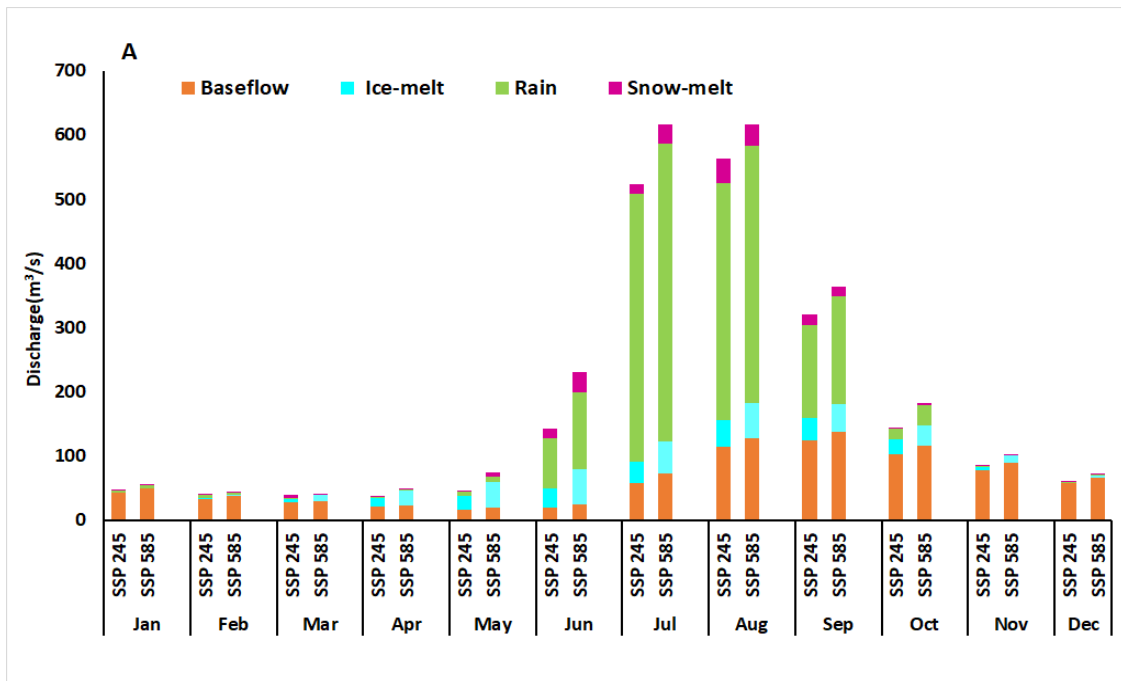


Figure 5. 8:(A) Monthly average simulated discharge during reference time period 2023-2030,2031-2040 and 2041-2050 under SSP24.5(B) Monthly average simulated discharge during reference time period 2023-2030,2031-2040 and 2041-2050 under SSP58.5

Figure 5.8 portrays noticeable information on shift in peak discharge pattern. For the period of 2023-2040 the peak discharge is at month of August as similar to baseline period with variation in discharge value, however there is shift in peak discharge to July with the discharge value higher than previous years at SSP24.5 scenarios. Similarly, in SSP58.5 scenarios the peak discharge shifts from August to month of July with higher discharge

value after 2030 onwards. The simulated monthly average discharge shows varying peak values during different time periods: from 2023-2050, peak discharge changes from 600 m³/s to 570 m³/s and then to 630 m³/s. Similarly, under the SSP5-8.5 scenario, the peak discharge evolves from 570 m³/s to 665 m³/s and further to 770 m³/s across these time frames. Here result of EC-Earth is heightened of among three GCM EC-Earth3 has the highest resolution of all three which tries in representing the actual physical climatic characteristics more accurately.



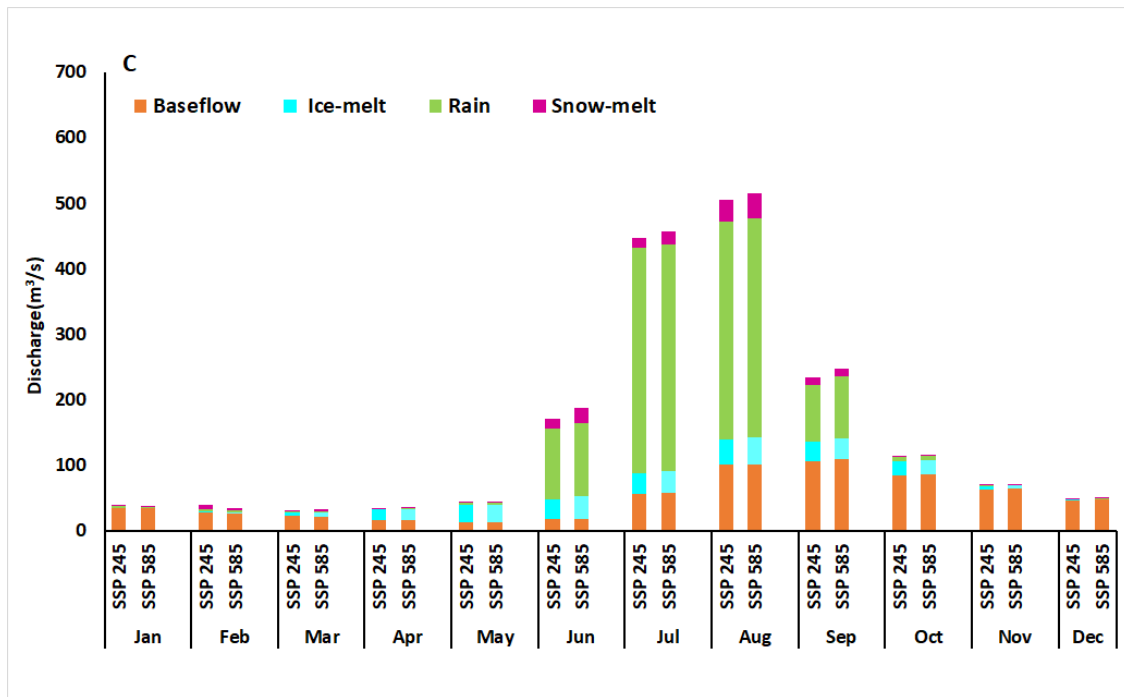


Figure 5. 9:(A) Average monthly contribution of hydrological components on discharge in SSP24.5 And SSP58.5 scenarios project by GCM EC-Earth3 for the period (2023-2050) .(B) Average monthly contribution of hydrological components on discharge in SSP24.5 And SSP58.5 scenarios project by GCM MPI-ESM1-2HR for the period (2023-2050) .(C) Average monthly contribution of hydrological components on discharge in SSP24.5 And SSP58.5 scenarios project by GCM Nor ESM2-MM for the period (2023-2050).

Figure 5.9 depicts the average monthly contributions of key factors affecting stream discharge between 2023 and 2050 in two distinct future scenarios, SSP24.5 and SSP58.5, as projected by three different GCMs. Across all GCM projections, the period from June to September consistently demonstrates rain as the primary contributor to stream flow, followed by base flow, snow melt, and ice melt. The baseflow contribution starts to peak from September with withdrawal of monsoon. Ice melt is noticeable from April to October across all three GCMs. The snow melt also happens to show its contribution from June to September during monsoon and start of post monsoon. In MPI-ESM1-2HR and Nor ESM2-MM under both SSP24.5 and SSP58.5 scenarios, the variations in the major hydrological parameters are quite similar. However, with EC-Earth3 in the SSP58.5 scenarios, total discharge surpasses that of the SSP24.5 scenarios due to differences in the value ranges of contributing components to stream flow. Across all three GCMs' future projections, rainfall and base flow remain the primary sources of stream flow in the upcoming years. On comparing obtained result with research study done on Koshi river

basin by (Khadka et al., 2020) the snow melt contribution is showing a decrease in stream contribution after which is reasonable considering the fact that snow-covered area and snow storage capacity decrease with increasing temperature, hence, decreased snow melt in the future. The ice melt contribution in Sunkoshi seems to be decreasing in RCP 8.5 scenario compared to RCP 4.5 in almost all the seasons and it might be due to the large reduction in glacier area in the basin for RCP 8.5 scenario. In our study the result varies from resulted provided in our study the contribution of Icemelt is in steady it might be because the consideration of change in glacier area retreat with respect to time is lagging in this research which is also stated in recommendation to obtain good in future research to perform. It should be noted that research shows a substantial decrease in glacier area in all the sub-basins, despite this there is still a significant contribution from ice melt in the future, which signifies rapid melting in the sub-basins that could result in a complete disappearance of glaciers (Khadka et al., 2020) in our study too the contribution of ice-melt is sows the significant ranges of contribution on stream flows in the future too.

CHAPTER SIX: CONCLUSION AND RECOMMENDATION

6.1 Conclusions

The Glacio-hydrological Degree-day Model (GDM) has been skillfully applied to Sunkoshi River basin to estimate discharge. This model provides valuable insights into the intricate hydrological dynamics of these basins, encompassing factors such as snowmelt, icemelt, rainfall, and baseflow contributions. Remarkably, despite its simplicity, the model consistently demonstrates its ability to faithfully replicate discharge patterns during both the calibration and validation periods. Notably, the Nash-Sutcliffe Efficiency (NSE) values for these river basins consistently fall within the range of 0.79 to 0.77, volume difference around -8 to -9.8 %, while the R-squared (R^2) value remains strong at around 0.83 to 0.77, underscoring its impressive performance. The examination focuses on discharge components in SRB. Snowmelt contributes 9.68% and 11.38% during calibration and validation, respectively. Clean ice and ice melt beneath debris make up 2.5% and 3%. Rainfall constitutes 50.15% and 48.26%, while baseflow accounts for 37.66% and 37.33% during these periods. During the low-flow period between April and June, the study demonstrates the significant contribution of snow and ice melt to river discharge during calibration and validation. Future analyses also indicate a noteworthy increase in ice melt's contribution compared to the base period, particularly during low-flow periods, highlighting its significant impact on stream flow. However, rising temperatures cause snowfall and existing glacier cover to decline, leading to a negative impact on the contribution of ice and snowmelt. This decline results in a serious impact on stream flow during future low-flow periods.

Temperature and precipitation trends differ notably between models across various scenarios. In SSP24.5, while EC-Earth3 indicates no significant trend, MPI-ESM1-2HR and Nor-ESM2-MM showcase varying increases in temperature, with rates at 0.03°C/year and 0.045°C/year, respectively. In SSP58.5, EC-Earth3 predicts a marked rise in temperature at 0.063°C/year, MPI-ESM1-2HR remains steady at 0.019°C/year, and Nor-ESM2-MM displays a contrasting decline. Future analysis of average monthly discharge under SSP24.5 between 2023 and 2040 shows peak discharge occurring in August, mirroring the baseline period, albeit with fluctuating discharge values. However, a shift in peak discharge from August to July is observed for the period 2040-2050. Similarly, in the SSP58.5 scenarios, the peak discharge transitions from August to July, with higher discharge values after 2030. The model's projections for future water scenarios reveal an

anticipated increase in discharge for river basins under the SSP58.5 scenarios. This increase is most pronounced, with values of 3.22 m³/s projected under EC-Earth3, followed by 0.55 m³/s under MPI-ESM1-2HR and 0.146 m³/s under Nor-ESM2-MM GCMs. In contrast, under the SSP 245 scenarios, the model forecasts a decrease in discharge for river basins. This decline is particularly notable, with values of 0.39 m³/s projected under MPI-ESM1-2HR, 0.33 m³/s under Nor-ESM2-MM, and 0.08 m³/s under EC-Earth3. The absence of an increase in discharge in these scenarios may be attributed to a decrease in precipitation and an increase in temperatures within the SSP24.5 scenarios. Future water scenarios, as depicted by different shared socio-environmental pathways (SSP24.5 and SSP58.5), showcase substantial variations in constituent contributions to overall discharge. Under SSP24.5, the breakdown reveals baseflow ranging from 32.99% to 34.04%, ice-melt spanning 10% to 13.37%, rainfall fluctuating from 46.51% to 51.13%, and snowmelt maintaining a smaller proportion between 4.84% and 6.66%. In contrast, within the SSP58.5 scenarios, baseflow contributions trend slightly upwards, ranging from 31.62% to 32.07%. Ice-melt proportions elevate notably to 14% to 18.12%, while rainfall remains relatively stable, varying from 44.56% to 48.8%. Similarly, snowmelt proportions remain consistent, ranging between 5.13% and 5.71%. These variations emphasize the potential alterations in resource availability and distribution across distinct future socio-environmental pathways.

In light of these findings, the GDM stands as a promising tool for investigating the dynamic nature of the hydrological system and for assessing the potential impacts of climate change on the Himalayan river basins.

6.2 Recommendation

To improve the GDM's accuracy in glacierized river basins, consider integrating glacier retreat modeling using OGGM. This data, including annual retreat rates and changes in ice area, significantly enhances GDM precision. It is advisable to model changes in settlement areas, forest cover, agricultural land, barren land, and wetlands. Incorporating data related to these land use and land cover changes into the GDM can yield more precise and reliable outcomes. Conducting an Isotope test can effectively scrutinize the roles played by rain, snowmelt, ice melt, and baseflow in the basin's stream flow contribution.

7. REFERENCES

- Adnan, M., Kang, S. change, Zhang, G. shuai, Anjum, M. N., Zaman, M., & Zhang, Y. qing. (2019). Evaluation of SWAT Model performance on glaciated and non-glaciated subbasins of Nam Co Lake, Southern Tibetan Plateau, China. *Journal of Mountain Science*, 16(5), 1075–1097. <https://doi.org/10.1007/s11629-018-5070-7>
- Bajracharya, S. R., Pradhananga, S., Shrestha, A. B., & Thapa, R. (2023). Future climate and its potential impact on the spatial and temporal hydrological regime in the Koshi Basin, Nepal. *Journal of Hydrology: Regional Studies*, 45. <https://doi.org/10.1016/j.ejrh.2023.101316>
- Barrios, A., Trincado, G., & Garreaud, R. (2018). Alternative approaches for estimating missing climate data: Application to monthly precipitation records in south-central Chile. *Forest Ecosystems*, 5(1). <https://doi.org/10.1186/s40663-018-0147-x>
- Barry, R. G. (2012). Recent advances in mountain climate research. *Theoretical and Applied Climatology*, 110(4), 549–553. <https://doi.org/10.1007/s00704-012-0695-x>
- Bharati, L., Bhattarai, U., Khadka, A., Gurung, P., Neumann, L. E., Penton, D. J., Dhaubanjari, S., & Nepal, S. (2019). From the mountains to the plains: Impact of climate change on water resources in the Koshi River Basin. *IWMI Working Papers*, 187, 1–54. <https://doi.org/10.5337/2019.205>
- Bocchiola, D., Diolaiuti, G., Soncini, A., Mihalcea, C., D'Agata, C., Mayer, C., Lambrecht, A., Rosso, R., & Smiraglia, C. (2011). Prediction of future hydrological regimes in poorly gauged high altitude basins: The case study of the upper Indus, Pakistan. *Hydrology and Earth System Sciences*, 15(7), 2059–2075. <https://doi.org/10.5194/hess-15-2059-2011>
- Braithwaite, R. J. (1995). Positive degree-day factors for ablation on the Greenland ice sheet studied by energy-balance modelling. *Journal of Glaciology*, 41, 153–160.
- Braithwaite, R. J., & Olesen, O. B. (1989). CALCULATION OF GLACIER ABLATION FROM AIR TEMPERATURE, WEST GREENLAND ABSTRACT.
- Braithwaite, R. J., & Olesen, O. B. (1990). Response of the energy balance on the margin of the Greenland ice sheet to temperature changes. *Journal of Glaciology*, 36(123), 217–221. <https://doi.org/10.1017/S0022143000009461>
- da Silva, M. G., de Aguiar Netto, A. de O., de Jesus Neves, R. J., do Vasco, A. N., Almeida, C., & Faccioli, G. G. (2015). Sensitivity Analysis and Calibration of Hydrological Modeling of the Watershed Northeast Brazil. *Journal of Environmental Protection*,

- 06(08), 837–850. <https://doi.org/10.4236/jep.2015.68076>
- Dai, A. (2011). Drought under global warming: A review. *Wiley Interdisciplinary Reviews: Climate Change*, 2(1), 45–65. <https://doi.org/10.1002/wcc.81>
- Devkota, L. P., & Gyawali, D. R. (2015). Impacts of climate change on hydrological regime and water resources management of the Koshi River Basin, Nepal. *Journal of Hydrology: Regional Studies*, 4, 502–515. <https://doi.org/10.1016/j.ejrh.2015.06.023>
- Droogers, P., Immerzeel, W. W., Terink, W., Hoogeveen, J., Bierkens, M. F. P., Van Beek, L. P. H., & Debele, B. (2012). Water resources trends in Middle East and North Africa towards 2050. *Hydrology and Earth System Sciences*, 16(9), 3101–3114. <https://doi.org/10.5194/hess-16-3101-2012>
- Githui, F., Mutua, F., & Bauwens, W. (2009). Estimating the impacts of land-cover change on runoff using the soil and water assessment tool (SWAT): Case study of Nzoia catchment, Kenya. *Hydrological Sciences Journal*, 54(5), 899–908. <https://doi.org/10.1623/hysj.54.5.899>
- Gupta, A., Kayastha, R. B., Ramanathan, A., & Dimri, A. P. (2019). Comparison of hydrological regime of glacierized Marshyangdi and Tamor river basins of Nepal. *Environmental Earth Sciences*, 78(14). <https://doi.org/10.1007/s12665-019-8443-5>
- Hassan, J., Chen, X. qing, Kayastha, R. B., & Nie, Y. (2021). Multi-model assessment of glacio-hydrological changes in central Karakoram, Pakistan. *Journal of Mountain Science*, 18(8), 1995–2011. <https://doi.org/10.1007/s11629-021-6748-9>
- Hock, R. (2003). Temperature index melt modelling in mountain areas. *Journal of Hydrology*, 282(1–4), 104–115. [https://doi.org/10.1016/S0022-1694\(03\)00257-9](https://doi.org/10.1016/S0022-1694(03)00257-9)
- ICIMOD. (2014). Glacier Status in Nepal and Decadal Change from 1980 to 2010 Based on Landsat Data 1.
- Immerzeel, W. W., Van Beek, L. P. H., & Bierkens, M. F. P. (2010). Climate change will affect the asian water towers. *Science*, 328(5984), 1382–1385. <https://doi.org/10.1126/science.1183188>
- Immerzeel, W. W., van Beek, L. P. H., Konz, M., Shrestha, A. B., & Bierkens, M. F. P. (2012). Hydrological response to climate change in a glacierized catchment in the Himalayas. *Climatic Change*, 110(3–4), 721–736. <https://doi.org/10.1007/s10584-011-0143-4>
- Immerzeel, W. W., Wanders, N., Lutz, A. F., Shea, J. M., & Bierkens, M. F. P. (2015). Reconciling high-altitude precipitation in the upper Indus basin with glacier mass balances and runoff. *Hydrology and Earth System Sciences*, 19(11), 4673–4687.

<https://doi.org/10.5194/hess-19-4673-2015>

IPCC. (2022). High Mountain Areas. In *The Ocean and Cryosphere in a Changing Climate*.

<https://doi.org/10.1017/9781009157964.010>

Jansson, P., Hock, R., & Schneider, T. (2003). The concept of glacier storage : a review.

282, 116–129. [https://doi.org/10.1016/S0022-1694\(03\)00258-0](https://doi.org/10.1016/S0022-1694(03)00258-0)

Kayastha, R. B., Ageta, Y., & Fujita, K. (2006). Use of Positive Degree-Day Methods for Calculating Snow and Ice Melting and Discharge in Glacierized Basins in the Langtang Valley, Central Nepal. *Climate and Hydrology in Mountain Areas*, 5–14.

<https://doi.org/10.1002/0470858249.ch2>

Kayastha, R. B., Ageta, Y., & Nakawo, M. (2000). Positive degree-day factors for ablation on glaciers in the Nepalese Himalayas: case study on Glacier AX010 in Shorong Himal, Nepal. *Bulletin of Glaciological Research*, 17, 1–10.

Kayastha, R. B., & Kayastha, R. (2019). Glacio-hydrological degree-day model (gdm) useful for the himalayan river basins. *Himalayan Weather and Climate and Their Impact on the Environment*, 379–398. https://doi.org/10.1007/978-3-030-29684-1_19

Kayastha, R. B., Steiner, N., Kayastha, R., Mishra, S. K., & McDonald, K. (2020). Comparative Study of Hydrology and Icemelt in Three Nepal River Basins Using the Glacio-Hydrological Degree-Day Model (GDM) and Observations From the Advanced Scatterometer (ASCAT). *Frontiers in Earth Science*, 7. <https://doi.org/10.3389/feart.2019.00354>

Khadka, A., Devkota, L. P., & Kayastha, R. B. (2015). Impact of Climate Change on the Snow Hydrology of Koshi River Basin. In *Journal of Hydrology and Meteorology* (Vol. 9, Issue 1).

Khadka, M., Kayastha, R. B., & Kayastha, R. (2020). Future projection of cryospheric and hydrologic regimes in Koshi River basin, Central Himalaya, using coupled glacier dynamics and glacio-hydrological models. *Journal of Glaciology*, 66(259), 831–845. <https://doi.org/10.1017/jog.2020.51>

Khanal, S., Lutz, A. F., Kraaijenbrink, P. D. A., van den Hurk, B., Yao, T., & Immerzeel, W. W. (2021). Variable 21st Century Climate Change Response for Rivers in High Mountain Asia at Seasonal to Decadal Time Scales. *Water Resources Research*, 57(5), 1–26. <https://doi.org/10.1029/2020WR029266>

Luo, Y., Arnold, J., Allen, P., & Chen, X. (2012). Baseflow simulation using SWAT model in an inland river basin in Tianshan Mountains, Northwest China. *Hydrology and*

- Earth System Sciences, 16(4), 1259–1267. <https://doi.org/10.5194/hess-16-1259-2012>
- Mishra, V., Bhatia, U., & Tiwari, A. D. (2020). Bias-corrected climate projections for South Asia from Coupled Model Intercomparison Project-6. *Scientific Data*, 7(1), 1–13. <https://doi.org/10.1038/s41597-020-00681-1>
- NAP. (2021). National Adaption Plan (NAP) 2021-2050: Nepal.
- Nash, J. E., & Sutcliffe, J. V. (1970). River Flow Forecasting Through Conceptual Models - Part I - A Discussion of Principles. *Journal of Hydrology*, 10(1970), 282–290.
- Niroula, N., Kobayashi, K., & Xu, J. (2015). Sunshine duration is declining in nepal across the period from 1987 to 2010. *Journal of Agricultural Meteorology*, 71(1), 15–23. <https://doi.org/10.2480/agrmet.D-14-00025>
- Ohmura, A. (2001). Physical basis for the temperature-based melt-index method. *Journal of Applied Meteorology*, 40(4), 753–761. [https://doi.org/10.1175/1520-0450\(2001\)040<0753:PBFTTB>2.0.CO;2](https://doi.org/10.1175/1520-0450(2001)040<0753:PBFTTB>2.0.CO;2)
- Pandey, V. P., Dhaubanjari, S., Bharati, L., & Thapa, B. R. (2020). Spatio-temporal distribution of water availability in Karnali-Mohana Basin, Western Nepal: Hydrological model development using multi-site calibration approach (Part-A). *Journal of Hydrology: Regional Studies*, 29. <https://doi.org/10.1016/j.ejrh.2020.100690>
- Pechlivanidis, I. G., Jackson, B. M., McIntyre, N. R., & Wheater, H. S. (2011). Catchment scale hydrological modelling: A review of model types, calibration approaches and uncertainty analysis methods in the context of recent developments in technology and applications. *Global Nest Journal*, 13(3), 193–214. <https://doi.org/10.30955/gnj.000778>
- Piani, C., Haerter, J. O., & Coppola, E. (2010). Statistical bias correction for daily precipitation in regional climate models over Europe. *Theoretical and Applied Climatology*, 99(1–2), 187–192. <https://doi.org/10.1007/s00704-009-0134-9>
- Rockström, J., Falkenmark, M., Lannerstad, M., & Karlberg, L. (2012). The planetary water drama: Dual task of feeding humanity and curbing climate change. *Geophysical Research Letters*, 39(15). <https://doi.org/10.1029/2012GL051688>
- Roy, L., Leconte, R., Brissette, F. P., & Marche, C. (2001). The impact of climate change on seasonal floods of a Southern Quebec river basin. *Hydrological Processes*, 15(16), 3167–3179. <https://doi.org/10.1002/hyp.323>
- Sattari, M. T., Rezazadeh-Joudi, A., & Kusiak, A. (2017). Assessment of different methods

- for estimation of missing data in precipitation studies. *Hydrology Research*, 48(4), 1032–1044. <https://doi.org/10.2166/nh.2016.364>
- Shrestha, A. B., Eriksson, M., Mool, P., Ghimire, P., Mishra, B., & Khanal, N. R. (2010a). Glacial lake outburst flood risk assessment of Sun Koshi basin, Nepal. *Geomatics, Natural Hazards and Risk*, 1(2), 157–169. <https://doi.org/10.1080/19475701003668968>
- Shrestha, A. B., Eriksson, M., Mool, P., Ghimire, P., Mishra, B., & Khanal, N. R. (2010b). Glacial lake outburst flood risk assessment of Sun Koshi basin, Nepal. *Geomatics, Natural Hazards and Risk*, 1(2), 157–169. <https://doi.org/10.1080/19475701003668968>
- Shrestha, S., Shrestha, M., & Babel, M. S. (2016). Modelling the potential impacts of climate change on hydrology and water resources in the Indrawati River Basin, Nepal. *Environmental Earth Sciences*, 75(4), 1–13. <https://doi.org/10.1007/s12665-015-5150-8>
- Teegavarapu, R. S. V., & Chandramouli, V. (2005). Improved weighting methods, deterministic and stochastic data-driven models for estimation of missing precipitation records. *Journal of Hydrology*, 312(1–4), 191–206. <https://doi.org/10.1016/j.jhydrol.2005.02.015>
- Wijngaard, R. R., Lutz, A. F., Nepal, S., Khanal, S., Pradhananga, S., Shrestha, A. B., & Immerzeel, W. W. (2017). Future changes in hydro-climatic extremes in the upper indus, ganges, and brahmaputra river basins. *Plos One*.
- WMO. (1986). Intercomparison of Models of Snowmelt. Operational Hydrology Report No. 23, WMO No. 646, 23, 482.
- Yang, M., Li, Z., Anjum, M. N., Kayastha, R., Kayastha, R. B., Rai, M., Zhang, X., & Xu, C. (2022). Projection of Streamflow Changes Under CMIP6 Scenarios in the Urumqi River Head Watershed, Tianshan Mountain, China. *Frontiers in Earth Science*, 10. <https://doi.org/10.3389/feart.2022.857854>
- Zhang, H., Zhang, F., Zhang, G., & Che, T. (2018). How accurately can the air temperature lapse rate over the Tibetan Plateau be estimated from MODIS LSTs ? *Journal of Geophysical Research : Atmospheres* How Accurately Can the Air Temperature Lapse Rate Over the Tibetan Plateau Be Estimated From MODIS LSTs. June 2019. <https://doi.org/10.1002/2017JD028243>
- Zhang, Y., Hirabayashi, Y., Liu, Q., & Liu, S. (2015). Glacier runoff and its impact in a highly glacierized catchment in the southeastern Tibetan Plateau: Past and future

trends. Journal of Glaciology, 61(228), 713–730.
<https://doi.org/10.3189/2015JoG14J188>

Simulation of streamflow in Glacierized Sunkoshi River Basin, Nepal, using a Glacio Hydrological Model

Sailesh Budhathoki^a, *Rijan Bhakta Kayastha*^b

Abstract:

The Glacio-hydrological Degree-day Model (GDM, Version 2.0) simulates the river runoff and dissects the contribution from different water balance components on simulated stream runoff. GDM has been setup in Sunkoshi river basin and quantifies the various component of river runoff. Initially model is calibrated for the period 2000-2009 and then validated for the period 2010-2020 and demonstrates a satisfactory level of accuracy during both calibration and validation periods, with Nash–Sutcliffe Efficiency (NSE) values 0.79 and 0.77, volume difference (V.D) 8%,9.8% and R2 0.8. In Sunkoshi river basin, of total runoff snowmelt accounts for 9.68% during calibration and 11.38% during validation. Clean ice and debris-covered ice contribute 2.5% and 3%, respectively. Rainfall accounts 50.15% during calibration and 48.26% during validation, while base flow contributes 37.66% during calibration and 37.33% during validation. Runoff contributions by different component is varied, rainfall dominates during the monsoon season (June–September) in river basins, while ice melt peaks from May to October, influenced by temperature and precipitation patterns. The model can be an effective tool for research work on hydrological system dynamics and potential climate change impacts on Himalayan river basins.

Keywords:

Climate change, Degree day factor, Glacier modelling, Glacio-Hydrological degree day model, Sunkoshi River Basin

^a Department of Applied Science and Chemical Engineering, Pulchowk campus, IOE, Tribhuvan University, Nepal

^b Department of Environmental Science and Engineering, School of Science, Himalayan Cryosphere, Climate and Disaster Research Center (HiCCDRC), Kathmandu University, Dhulikhel, Nepal

✉ ^a Sailesh093@gmail.com, ^b rijan@KU.edu.np



IOE Graduate Conference


Certificate of Participation





This certificate is awarded to
Sailesh Budhathoki

in recognition of an invaluable contribution as
Poster Presenter
at the **14th IOE Graduate Conference**

Organized by Tribhuvan University, IOE, Curriculum and Instructional Material
Development Unit (CIMDU) held from November 29 to December 1, 2023 at
Pulchowk Campus, Lalitpur, Nepal.


Ast. Prof. Bhim Kumar Dahal, PhD
Conference Convener


Assoc. Prof. Indra Prasad Acharya, PhD
Campus Chief
Pulchowk Campus


Prof. Shashidhar Ram Joshi, PhD
Dean
Institute of Engineering

15%

SIMILARITY INDEX

PRIMARY SOURCES

1	www.cambridge.org Internet	209 words — 1%
2	sarahrshannon.github.io Internet	202 words — 1%
3	www.frontiersin.org Internet	201 words — 1%
4	elibrary.tucl.edu.np Internet	99 words — 1%
5	www.researchgate.net Internet	86 words — 1%
6	www.tandfonline.com Internet	69 words — < 1%
7	etd.aau.edu.et Internet	57 words — < 1%
8	Laxmi Prasad Devkota, Dhiraj Raj Gyawali. "Impacts of climate change on hydrological regime and water resources management of the Koshi River Basin, Nepal", Journal of Hydrology: Regional Studies, 2015 Crossref	56 words — < 1%
9	d-nb.info Internet	